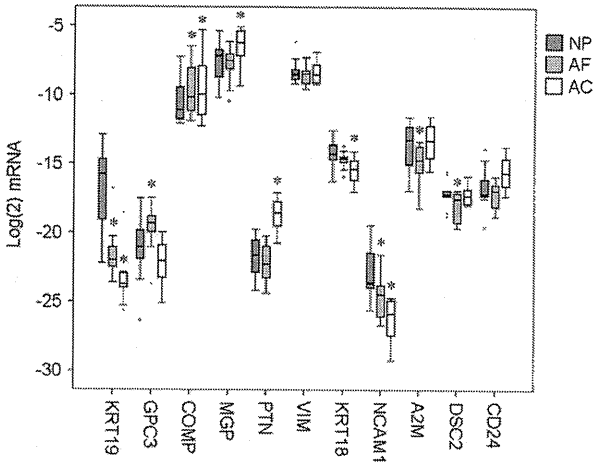

Fig. 1. Relative mRNA expression in human NP, AF, and AC cells. Expression levels were normalized to 18S rRNA as the endogenous control. *$P < 0.05$ in pair-wise comparison of NP with corresponding AF or AC; N = 9–11.

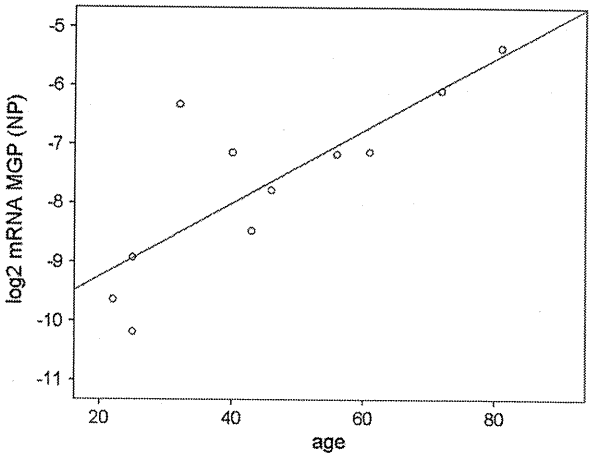

Fig. 3. Relative mRNA expression for MGP in NP cells of 11 individuals between 22 and 81 years of age. Gene expression was normalized to the 18S ribosomal RNA. An increase in the MGP expression level with increasing age is noted.

expression levels of GPC3 and cartilage oligomeric matrix protein (COMP) were higher in the AF compared to the NP, whereas COMP, MGP, and pleiotrophin (PTN) were expressed more highly in the AC than in the NP cells. No differences in vimentin (VIM) and Cluster of Differentiation 24 antigen (CD24) expression were noted between NP and AF or AC cells (Fig. 1).

While the KRT19 expression of AC and AF cells did not change throughout age groups, its expression in the NP cells showed a decrease with age ($P = 0.032$; Fig. 2). However, in spite of this decrease, KRT19 was still more highly expressed in the NP compared to the AF and AC cells even in older individuals. A correlation between age and gene expression in NP cells was also found for MGP mRNA, which increased with increasing age ($P = 0.003$; Fig. 3). In the AF cells, increasing levels of PTN mRNA were noted with aging ($P = 0.023$; data not shown). The expression of MGP in NP cells was also positively correlated with the degree of degeneration ($P = 0.007$). The relation between KRT19 level in the NP and degeneration grade was found to be almost significant ($P = 0.061$). No association between age or degeneration grade and the level of expression was detected with any of the other genes analysed. However, in agreement with previous reports, there was a strong relationship between age and degeneration grade of the disc ($P < 0.001$).

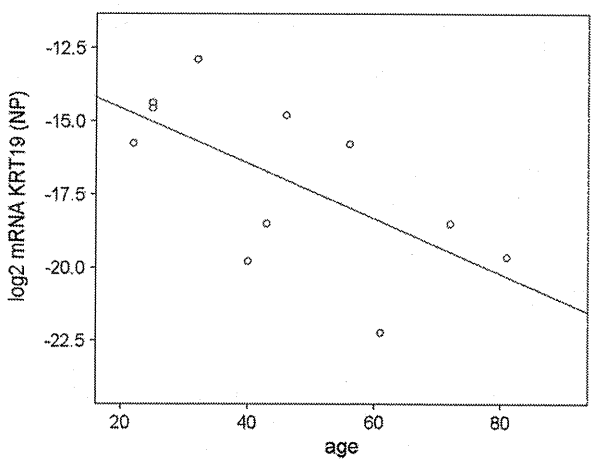

Fig. 2. Relative mRNA expression for KRT19 in NP cells of 11 individuals between 22 and 81 years of age. Gene expression was normalized to the 18S ribosomal RNA. A decrease in the KRT19 expression level with increasing age is noted.

IMMUNOHISTOCHEMISTRY

KRT19 was chosen for immunohistochemical analysis, since this molecule showed most pronounced differences between NP and AF or AC with respect to mRNA expression, whereas MGP was selected for analysis at the protein level because of its apparent age- and degeneration-dependent increase in the NP cells, which are of main interest in this study.

In the NP of juvenile discs (<5 years of age), clusters of large cells with a notochordal morphology were identified. These cells were positive for KRT19 [Fig. 4(A)], while neither cells within the AF nor cells of the cartilaginous endplate revealed any positive labelling [Fig. 4(B), Table III]. In the NP of young discs with Thompson score 1 but without apparent existence of notochordal cells (age range 6–25 years), KRT19 positive cells were observed in 60% ($n = 6/10$) of the individuals. Labelling was located predominantly intracellular and was limited to a small number of cells that had a somewhat chondrocytic appearance with no morphological evidence of a notochordal cell phenotype [Fig. 4(C, D)]. On the other hand, the majority of healthy adult discs did not reveal any immunoreactivity for KRT19 [Fig. 4(E)]. In two degenerate discs however (patients with sepsis), positive cells were detected adjacent to fissures associated with degenerative changes of the cartilaginous endplate [Fig. 4(G)]. These cells exhibited a characteristic chondrocyte-like morphology, were located at the border between cartilaginous endplate and NP and were not regarded as NP cells.

The number of MGP positive cells in general was higher than the number of KRT19 positive cells, but non labelled

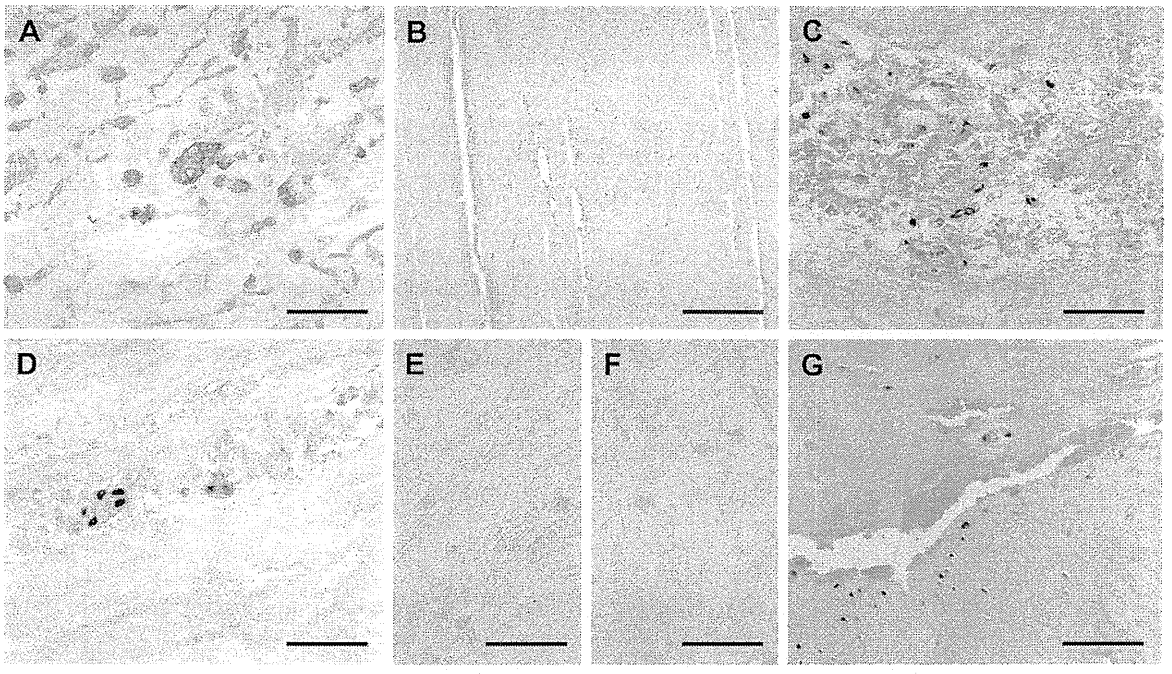

Fig. 4. Immunolabelling characteristics for KRT19. (A) Cells within the NP of a 3-year-old human female label positive for KRT19. (B) No KRT19 positive cells are detected in the inner annulus of a 21-year-old male individual. (C) A group of KRT19 positive cells in the NP of a 14-year-old male. (D) Small group of KRT19 positive cells from the NP of a 21-year-old male (same individual as in B). (E) NP of a 47-year-old female with Thompson grade 3. No positive labelling can be detected. (F) Control from same individual as in E. (G) 72-year-old male donor with disc degeneration grade 4. The image shows the edge of the NP region. The cartilaginous endplate is at the bottom of the image. Several KRT19 positive cells with a chondrocyte-like morphology can be detected. All scale bars = 100 μm.

cells clearly constitute the largest cell fraction. However, in juvenile and young adult discs positive cells could be detected in the NP (Table III). MGP positive cells were found in distinct clusters of NP cells in young individuals [Fig. 5(A, B)]. In older more degenerated discs (grade 3 and higher) positive cells were found adjacent to clefts and cracks [Fig. 5(D)]. Furthermore, the outer AF was often immunopositive [Fig. 5(E)], with a decreasing intensity towards the inner AF [Fig. 5(F)]. Labelling was limited to the cells and to a very small portion of the pericellular matrix in their immediate vicinity. The cells and extracellular matrix of the mineralized cartilage of the endplate often demonstrated a positive reaction for MGP, especially at the tidemark [Fig. 5(G, H)]. The non-mineralized cartilage of the endplate was always negative [Fig. 5(G, H)]. The fibrocartilaginous attachment of the outer AF frequently labelled positive [Fig. 5(I)].

Discussion

Degenerative changes occurring in the IVD have been extensively described and mechanisms, including genetic variations that may cause a predisposition to IVD degeneration are being elucidated. However, the molecular profile that characterizes the normal disc, and in particular the NP cell is still unknown. Previous investigations have suggested potential markers for IVD cells and more specifically for NP cells[7,8,13,17]. The present study is a further contribution to the identification of molecules expressed in human disc cells. It was undertaken to validate potential NP marker molecules identified by large scale gene expression screening in the rat and dog for their potential use with human cells.

Looking at genes previously identified as markers for the rat NP, the expression of KRT19 could be confirmed for human cells. However, a decrease in KRT19 expression with age was noted in the NP, while the expression in AF and AC remained constant. As KRT19 has also been associated with notochordal cells and chordoma, its expression in healthy adult human NP cells may be unexpected[18,19]. Indeed, immunohistochemical analysis confirmed its presence in cells with a notochordal phenotype and further supported the suggestion of an age-dependent expression pattern. At the protein level, KRT19 was barely detectable in the NP after the third decade, although mRNA expression was still clearly measurable. Possible explanations for this finding may include differences in the detection limit between mRNA and protein expression, instability of the mRNA, short protein half-life, or inhibition at the translational level.

In contrast to KRT19, the expression pattern of the other genes that had been found to be expressed more highly in the NP than in the AC in rat specimens, including CD24, was not confirmed in human samples[7,13]. However, GPC3 and PTN expression profiles were similar to observations in beagle dogs[8]. This might be related to the comparable development of the NP with respect to cell phenotype in human individuals and chondrodystrophoid dogs, which clearly differs from the development in rats. Looking at the genes evaluated for the beagle dog, the human samples generally showed a similar expression pattern, with higher levels of KRT18, A2M, and NCAM1 in NP vs AF and/or AC. Besides KRT19, only NCAM1 was expressed more

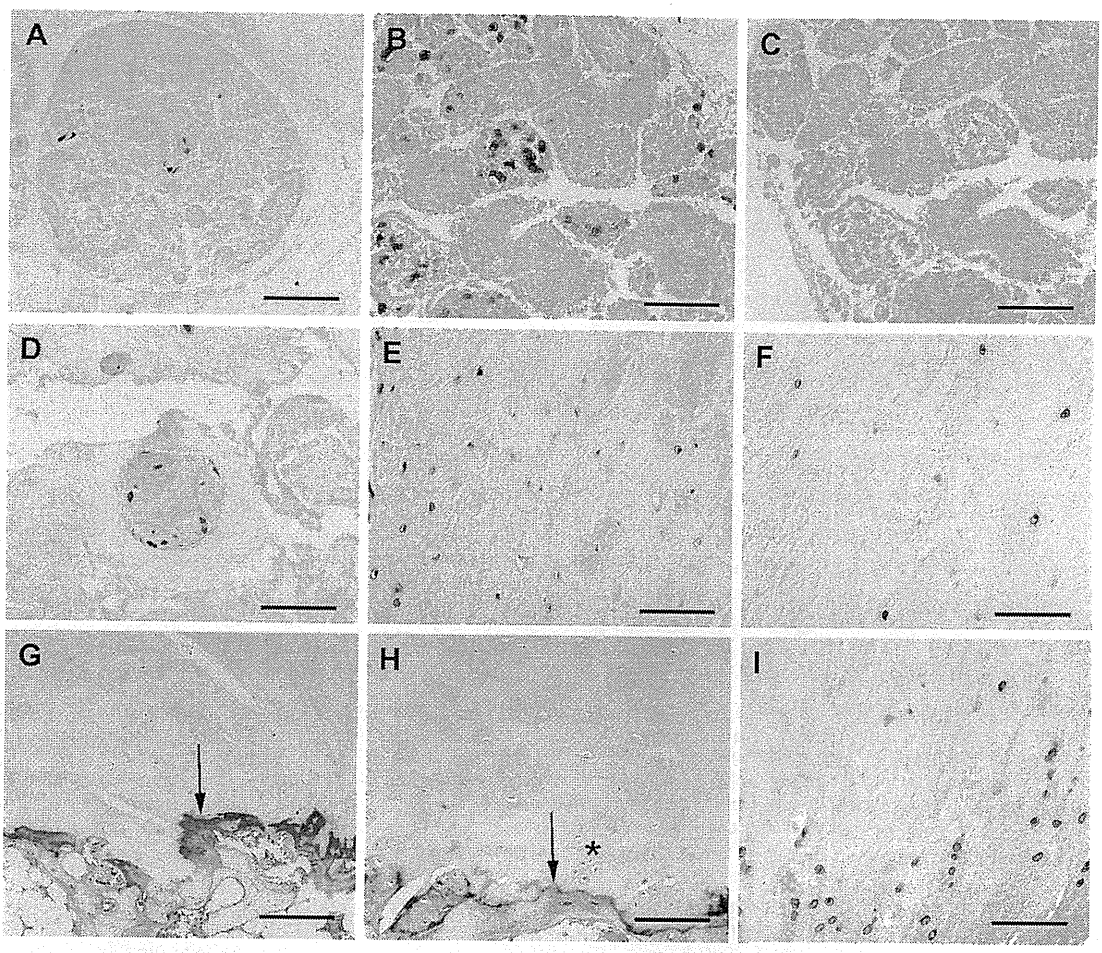

Fig. 5. Immunolabelling characteristics for MGP. (A) Cells within the NP of a 6-year-old human female label positive for MGP. (B) Group of MGP positive cells in the NP of a 17-year-old male. (C) Control from same individual and same region as shown in B. (D) Small group of MGP positive cells from the NP of a 60-year-old male individual with disc degeneration Thompson grade 5. Note that the cells are forming a cluster like structure in the neighbourhood of a fissure. (E) Outer and (F) inner annulus of a 35-year-old female with Thompson grade 2. Several positive cells can be detected. The surrounding extracellular matrix is negative. (G) Endplate cartilage from a 72-year-old male with Thompson grade 5. Note the strong positive labelling at the tidemark (arrow) and in the calcified cartilage. Cells in non-calcified cartilage are all negative. (H) Endplate cartilage from a 35-year-old female individual with Thompson grade 2. The positive labelling at the tidemark (arrow) is clearly visible. Cartilage cells form clusters (*) but are all negative. (I) Fibrocartilaginous attachment of the outer annulus of a 35-year-old female individual (same as in H). The fibrocartilage cells are arranged in characteristic rows and label positive for MGP. Scale bar in G = 200 μm, all other scale bars = 100 μm.

highly in NP than both AF and AC cells in this study. NCAM1 is an integral membrane glycoprotein that can regulate both cell–cell and cell–substrate interactions, primarily through polysialic acid[20,21]. Although it is expressed primarily in the nervous system, NCAM1 has been identified in various tissues in the adult rat[22]. In development NCAM1 plays a significant role in cell differentiation, including diverse functions in osteogenesis and chondrogenesis[23]. However, the fact that NCAM1 was expressed at a low level in all cell types analysed depreciates this molecule as a useful marker for human NP cells.

The matrix protein COMP showed consistently lower expression in NP than in AF and AC cells in all species. This differential expression of COMP in cartilage and disc adds to earlier observations of variations in the relative amounts of distinct matrix molecules in these two tissues[6]. While COMP has been identified and localized in the IVD, its relatively lower expression may reflect differences in the mechanical properties between the NP and cartilage tissues[24]. The main molecular functions of COMP include binding other matrix proteins and catalyzing polymerization of type II collagen fibrils. Furthermore, COMP is reported to prevent vascularization of cartilage and this could also be the case in the IVD tissues[25].

Commonly, work that addresses the disc cell profile leads to the conclusion that disc cells express a predominantly chondrocytic phenotype[26–28]. Investigations on mature bovine IVD cells agreed that NP cells produce more proteoglycans and less collagen than AF and cartilage cells, which is consistent with the higher hydration of the NP tissue[6,29]. In rat spinal units it was demonstrated that NP can be distinguished from adjacent tissues by the expression of proteins that are synthesized in response to restriction in oxygen and nutrient supply[17]. Additional studies in the rat revealed other potentially NP specific markers[7,13]. However, a major disadvantage of using rat NP is the presence of cells with

a notochordal phenotype. In fact several studies have used rat cells to explore the notochordal molecular phenotype in the disc[30,31]. Therefore, results from the rat, as well as mouse or rabbit have to be extrapolated with care to the human situation. Apart from the different developmental pathways of the NP cell populations the large deviations in IVD size and thus nutrition and mechanical conditions are also likely to influence the molecular characteristics of NP cells. Nevertheless, the expression profile of KRT19 demonstrates that selected genes may be valuable as markers even in different species.

When comparing the present study with previous studies on beagles, it also has to be noted that the human samples in this study are very heterogeneous with respect to age, while the animals all had the same age. This may explain the less pronounced differences between NP, AF, and cartilage cells in human individuals compared to the dog species, while general trends were identical in both species. Consequently, the age of the animal always has to be taken into consideration for the interpretation of results from an animal model. Moreover, although a study in the rat did not reveal major differences in gene expression pattern between RNA extracted from isolated cells and RNA extracted directly from the tissues, enzymatic cell isolation might have contributed to the reduced tissue-related differences observed in human specimens[7]. Besides, it is sometimes difficult to clearly distinguish human NP from AF tissue, especially in aged discs, which can also result in lowered gene expression differences between NP and AF cells. In view of these difficulties and the observed age-related alterations, young individuals are clearly preferred for the study of the phenotype of the healthy human NP cell.

Age-related changes have been detected regarding matrix composition, expression of matrix degrading enzymes, and other processes[3,6,32–34]. Although differences between aging and (early) degeneration were recently described in rabbits, a strong correlation exists between age and degeneration grade in human patients[3,35,36], which is confirmed in this study. Thus, it is not possible to clearly separate the influence of aging from that of degeneration mechanisms. Accordingly, Adams and Roughly defined a degenerate disc as one with structural failure combined with accelerated or advanced signs of aging[37]. This has recently been demonstrated also for the cervical spine, where in a longitudinal study no other factor except for age was related to the progression of degeneration[38]. Although cases of early disc degeneration have been described and are of particular value for specific investigation of degenerative processes, the present study evaluated individuals with "natural" disc development, where aging is accompanied with a certain degree of degeneration. This is particularly reflected in the mRNA expression of MGP in the NP, which strongly correlated with both aging and degree of degeneration. MGP is a Bone morphogenetic protein-2 (BMP-2) regulatory protein that is known as a calcification inhibitor in cartilage and in arteries[39,40]. Interestingly, MGP serum levels of community-based cohorts were also elevated with increasing age and were associated with individual risk factors for coronary heart disease[41]. It was suggested that induction of MGP expression may be a feedback mechanism to prevent mineralization of calcium deposits in the arteries[41]. Similarly, one could speculate that induction of MGP in the NP may be an attempt to prevent calcification processes that have been observed in the aging disc[42,43]. The presence of MGP in areas of mineralized cartilage in the endplate and in cells adjacent to sites of degeneration would support this hypothesis. The same is true for the expression at the fibrocartilaginous attachment of the outer AF where ectopic ossification (i.e., exophyte growth) would be prevented. Interestingly MGP expression in non-calcified AC is restricted to the superficial regions in monkeys and is barely detectable in senile human cartilage tissue[44]. In chondrocytic cells, both over-expression of MGP in maturing chondrocytes and under-expression of MGP in proliferative and hypertrophic chondrocytes may induce apoptosis[45]. As it has been reported that some cells of the IVD may differentiate towards the hypertrophic chondrocyte phenotype with age, MGP might function to prevent apoptosis in these cells[46]. Further studies are required to clarify the role of MGP expressed in the disc.

The observed rise in PTN gene expression in the AF with aging may result from a cellular attempt to restore a slowly degrading tissue. PTN functions as a growth and differentiation factor in many cell types and has been shown to induce the synthesis of matrix molecules in articular chondrocytes[47]. In cartilage, elevated PTN levels have been related to both osteoarthritis and rheumatoid arthritis[48,49]. Interestingly, an increased amount of PTN-immunopositive cells was observed in degenerated and in prolapsed disc samples and was associated with vascularization of diseased or damaged tissue[50]. Since blood vessels are mostly localized in the outer AF and rarely penetrate into deeper zones of the IVD, an increasing expression of PTN in the AF with aging would support the suggestion that PTN may function as an angiogenic factor in the degenerating IVD[50]. Age- or degeneration-associated changes might become clinically useful markers to determine the "juvenileness" or the regenerative capacity of IVD tissues sampled from discectomies or nucleotomies. More extended studies will be required to validate the potential of such markers to individually evaluate the most appropriate treatment of an IVD disorder.

In conclusion, from a selection of NP phenotype markers identified in animal studies, KRT19 and NCAM1 expression were found to be more pronounced in NP than AF and AC cells in human individuals. Whereas NCAM1 levels are relatively low even in NP cells, KRT19 may be regarded as a marker for human NP cells, being highly expressed in NP and at significantly lower levels in AF and AC cells. This observation on the subject of gene expression is at least partially reflected at the protein level, where KRT19 positive cells are almost exclusively identified in the NP of juvenile and young adult discs. This suggests that KRT19 transcripts are translated into detectable amounts of protein primarily in notochordal-like cells of juvenile NP and occasionally in young chondrocyte-like NP cells. MGP is found in a variety of human IVD tissues and thus cannot serve as a characteristic NP marker.

Conflict of interest

The authors confirm that they have no financial and personal relationships with other people or organisations that could inappropriately influence their work.

Acknowledgements

The authors acknowledge the Department of Pathology of the UMC Utrecht, in particular F. Bernhard and A. de Ruiter for their help in obtaining the IVD specimens.
This study was supported by the Swiss National Science Foundation (Grant #3320000-116818).

References

1. Waddell G. Low back pain: a twentieth century health care enigma. Spine 1996;21:2820–5.
2. Phelip X. Why the back of the child? Eur Spine J 1999;8:426–8.
3. Antoniou J, Steffen T, Nelson F, Winterbottom N, Hollander AP, Poole RA, *et al.* The human lumbar intervertebral disc: evidence for changes in the biosynthesis and denaturation of the extracellular matrix with growth, maturation, ageing, and degeneration. J Clin Invest 1996;98:996–1003.
4. Leung VY, Chan D, Cheung KM. Regeneration of intervertebral disc by mesenchymal stem cells: potentials, limitations, and future direction. Eur Spine J 2006;15(Suppl 3):S406–13.
5. Hiyama A, Mochida J, Sakai D. Stem cell applications in intervertebral disc repair. Cell Mol Biol (Noisy-le-grand) 2008;54:24–32.
6. Mwale F, Roughley P, Antoniou J. Distinction between the extracellular matrix of the nucleus pulposus and hyaline cartilage: a requisite for tissue engineering of intervertebral disc. Eur Cell Mater 2004;8:58–63.
7. Lee CR, Sakai D, Nakai T, Toyama K, Mochida J, Alini M, *et al.* A phenotypic comparison of intervertebral disc and articular cartilage cells in the rat. Eur Spine J 2007;16:2174–85.
8. Sakai D, Nakai T, Mochida J, Alini M, Grad S. Differential phenotype of intervertebral disc cells: microarray and immunohistochemical analysis of canine nucleus pulposus and anulus fibrosus. Spine 2009;34:1448–56.
9. Alini M, Eisenstein SM, Ito K, Little C, Kettler AA, Masuda K, *et al.* Are animal models useful for studying human disc disorders/degeneration? Eur Spine J 2008;17:2–19.
10. Hunter CJ, Matyas JR, Duncan NA. Cytomorphology of notochordal and chondrocytic cells from the nucleus pulposus: a species comparison. J Anat 2004;205:357–62.
11. Thompson JP, Pearce RH, Schechter MT, Adams ME, Tsang IK, Bishop PB. Preliminary evaluation of a scheme for grading the gross morphology of the human intervertebral disc. Spine 1990;15:411–5.
12. Reno C, Marchuk L, Sciore P, Frank CB, Hart DA. Rapid isolation of total RNA from small samples of hypocellular, dense connective tissues. Biotechniques 1997;22:1082–6.
13. Fujita N, Miyamoto T, Imai J, Hosogane N, Suzuki T, Yagi M, *et al.* CD24 is expressed specifically in the nucleus pulposus of intervertebral discs. Biochem Biophys Res Commun 2005;338:1890–6.
14. Livak KJ, Schmittgen TD. Analysis of relative gene expression data using real-time quantitative PCR and the 2(-Delta Delta C(T)) method. Methods 2001;25:402–8.
15. Lee CR, Grad S, MacLean JJ, Iatridis JC, Alini M. Effect of mechanical loading on mRNA levels of common endogenous controls in articular chondrocytes and intervertebral disk. Anal Biochem 2005;341:372–5.
16. Kristensen HK. An improved method of decalcification. Stain Technol 1948;23:151–4.
17. Rajpurohit R, Risbud MV, Ducheyne P, Vresilovic EJ, Shapiro IM. Phenotypic characteristics of the nucleus pulposus: expression of hypoxia inducing factor-1, glucose transporter-1 and MMP-2. Cell Tissue Res 2002;308:401–7.
18. Stosiek P, Kasper M, Karsten U. Expression of cytokeratin and vimentin in nucleus pulposus cells. Differentiation 1988;39:78–81.
19. Gottschalk D, Fehn M, Patt S, Saeger W, Kirchner T, Aigner T. Matrix gene expression analysis and cellular phenotyping in chordoma reveals focal differentiation pattern of neoplastic cells mimicking nucleus pulposus development. Am J Pathol 2001;158:1571–8.
20. Rutishauser U, Acheson A, Hall AK, Mann DM, Sunshine J. The neural cell adhesion molecule (NCAM) as a regulator of cell-cell interactions. Science 1988;240:53–7.
21. Acheson A, Sunshine JL, Rutishauser U. NCAM polysialic acid can regulate both cell–cell and cell–substrate interactions. J Cell Biol 1991; 114:143–53.
22. Filiz S, Dalcik H, Yardimoglu M, Gonca S, Ceylan S. Localization of neural cell adhesion molecule (N-CAM) immunoreactivity in adult rat tissues. Biotech Histochem 2002;77:127–35.
23. Fang J, Hall BK. N-CAM is not required for initiation of secondary chondrogenesis: the role of N-CAM in skeletal condensation and differentiation. Int J Dev Biol 1999;43:335–42.
24. Ishii Y, Thomas AO, Guo XE, Hung CT, Chen FH. Localization and distribution of cartilage oligomeric matrix protein in the rat intervertebral disc. Spine 2006;31:1539–46.
25. Hyc A, Osiecka-Iwan A, Jozwiak J, Moskalewski S. The morphology and selected biological properties of articular cartilage. Ortop Traumatol Rehabil 2001;3:151–62.
26. Chelberg MK, Banks GM, Geiger DF, Oegema Jr TR. Identification of heterogeneous cell populations in normal human intervertebral disc. J Anat 1995;186(Pt 1):43–53.
27. Sive JI, Baird P, Jeziorsk M, Watkins A, Hoyland JA, Freemont AJ. Expression of chondrocyte markers by cells of normal and degenerate intervertebral discs. Mol Pathol 2002;55:91–7.
28. Poiraudeau S, Monteiro I, Anract P, Blanchard O, Revel M, Corvol MT. Phenotypic characteristics of rabbit intervertebral disc cells. Comparison with cartilage cells from the same animals. Spine 1999;24: 837–44.
29. Horner HA, Roberts S, Bielby RC, Menage J, Evans H, Urban JP. Cells from different regions of the intervertebral disc: effect of culture system on matrix expression and cell phenotype. Spine 2002;27: 1018–28.
30. Chen J, Yan W, Setton LA. Molecular phenotypes of notochordal cells purified from immature nucleus pulposus. Eur Spine J 2006;15(Suppl 3):S303–11.
31. Oguz E, Tsai TT, Di Martino A, Guttapalli A, Albert TJ, Shapiro IM, *et al.* Galectin-3 expression in the intervertebral disc: a useful marker of the notochord phenotype? Spine 2007;32:9–16.
32. Le Maitre CL, Freemont AJ, Hoyland JA. Localization of degradative enzymes and their inhibitors in the degenerate human intervertebral disc. J Pathol 2004;204:47–54.
33. Le Maitre CL, Freemont AJ, Hoyland JA. Human disc degeneration is associated with increased MMP 7 expression. Biotech Histochem 2006;81:125–31.
34. Nerlich AG, Schleicher ED, Boos N. 1997 Volvo award winner in basic science studies. Immunohistologic markers for age-related changes of human lumbar intervertebral discs. Spine 1997;22:2781–95.
35. Sowa G, Vadala G, Studer R, Kompel J, Iucu C, Georgescu H, *et al.* Characterization of intervertebral disc aging: longitudinal analysis of a rabbit model by magnetic resonance imaging, histology, and gene expression. Spine 2008;33:1821–8.
36. Miller JA, Schmatz C, Schultz AB. Lumbar disc degeneration: correlation with age, sex, and spine level in 600 autopsy specimens. Spine 1988; 13:173–8.
37. Adams MA, Roughley PJ. What is intervertebral disc degeneration, and what causes it? Spine 2006;31:2151–61.
38. Okada E, Matsumoto M, Ichihara D, Chiba K, Toyama J, Fujiwara H, *et al.* Aging of the cervical spine in healthy volunteers: a 10-year longitudinal magnetic resonance imaging study. Spine 2009;34:706–12.
39. Luo G, Ducy P, McKee MD, Pinero GJ, Loyer E, Behringer RR, *et al.* Spontaneous calcification of arteries and cartilage in mice lacking matrix gla protein. Nature 1997;386:78–81.
40. Zebboudj AF, Imura M, Bostrom K. Matrix gla protein, a regulatory protein for bone morphogenetic protein-2. J Biol Chem 2002;277: 4388–94.
41. O'Donnell CJ, Shea MK, Price PA, Gagnon DR, Wilson PW, Larson MG, *et al.* Matrix gla protein is associated with risk factors for atherosclerosis but not with coronary artery calcification. Arterioscler Thromb Vasc Biol 2006;26:2769–74.
42. Cheng XG, Brys P, Nijs J, Nicholson P, Jiang Y, Baert AL, *et al.* Radiological prevalence of lumbar intervertebral disc calcification in the elderly: an autopsy study. Skeletal Radiol 1996;25:231–5.
43. Oda J, Tanaka H, Tsuzuki N. Intervertebral disc changes with aging of human cervical vertebra. From the neonate to the eighties. Spine 1988;13:1205–11.
44. Loeser R, Carlson CS, Tulli H, Jerome WG, Miller L, Wallin R. Articular-cartilage matrix gamma-carboxyglutamic acid-containing protein. Characterization and immunolocalization. Biochem J 1992; 282(Pt 1):1–6.
45. Newman B, Gigout LI, Sudre L, Grant ME, Wallis GA. Coordinated expression of matrix gla protein is required during endochondral ossification for chondrocyte survival. J Cell Biol 2001;154:659–66.
46. Aigner T, Gresk-otter KR, Fairbank JC, Von der Mark K, Urban JP. Variation with age in the pattern of type X collagen expression in normal and scoliotic human intervertebral discs. Calcif Tissue Int 1998;63: 263–8.
47. Tapp H, Hernandez DJ, Neame PJ, Koob TJ. Pleiotrophin inhibits chondrocyte proliferation and stimulates proteoglycan synthesis in mature bovine cartilage. Matrix Biol 1999;18:543–56.
48. Pufe T, Bartscher M, Petersen W, Tillmann B, Mentlein R. Pleiotrophin, an embryonic differentiation and growth factor, is expressed in osteoarthritis. Osteoarthritis Cartilage 2003;11:260–4.
49. Pufe T, Bartscher M, Petersen W, Tillmann B, Mentlein R. Expression of pleiotrophin, an embryonic growth and differentiation factor, in rheumatoid arthritis. Arthritis Rheum 2003;48:660–7.
50. Johnson WE, Patterson AM, Eisenstein SM, Roberts S. The presence of pleiotrophin in the human intervertebral disc is associated with increased vascularization: an immunohistologic study. Spine 2007;32: 1295–302.

European Cells and Materials Vol. 17 2009 (pages 15-22) ISSN 1473-2262

LOW-INTENSITY PULSED ULTRASOUND STIMULATES CELL PROLIFERATION, PROTEOGLYCAN SYNTHESIS AND EXPRESSION OF GROWTH FACTOR-RELATED GENES IN HUMAN NUCLEUS PULPOSUS CELL LINE

Yuka Kobayashi[1], Daisuke Sakai[1,2*], Toru Iwashina[1,2], Sadahiro Iwabuchi[3], and Joji Mochida[1,2]
[1]Department of Orthopaedic Surgery, Surgical Science,
[2]Research Center for Regenerative Medicine, Tokai University School of Medicine, 143 Shimokasuya, Isehara, Kanagawa, 259-1193, Japan
[3]Bio-medical Engineering Laboratories, Tejin Pharma Ltd., 3-2, Asahigaoka, 4-chome, Hino, Tokyo, 191-8512, Japan

Abstract

Low-intensity pulsed ultrasound (LIPUS) stimulation has been shown to effect differentiation and activation of human chondrocytes. A study involving stimulation of rabbit disc cells with LIPUS revealed upregulation of cell proliferation and proteoglycan (PG) synthesis. However, the effect of LIPUS on human nucleus pulposus cells has not been investigated. In the present study, therefore, we investigated whether LIPUS stimulation of a human nucleus pulposus cell line (HNPSV-1) exerted a positive effect on cellular activity. HNPSV-1 cells were encapsulated in 1.2% sodium alginate solution at $1x10^5$ cells/ml and cultured at 10 beads/well in 6-well plates. The cells were stimulated for 20 min each day using a LIPUS generator, and the effects of LIPUS were evaluated by measuring DNA and PG synthesis. Furthermore, mRNA expression was analyzed by cDNA microarray using total RNA extracted from the cultured cells. Our study revealed no significant difference in cell proliferation between the control and the ultrasound treated groups. However, PG production was significantly upregulated in HNPSV cells stimulated at intensities of 15, 30, 60, and 120 mW/cm^2 compared with the control. The results of cDNA array showed that LIPUS significantly stimulated the gene expression of growth factors and their receptors (BMP2, FGF7, TGFβR1 EGFRF1, VEGF). These findings suggest that LIPUS stimulation upregulates PG production in human nucleus pulposus cells by the enhancement of several matrix-related genes including growth factor-related genes. Safe and non-invasive stimulation using LIPUS may be a useful treatment for delaying the progression of disc degeneration.

Keywords: LIPUS, ultrasound, intervertebral disc, growth factor.

*Address for correspondence
Department of Orthopaedic Surgery/Surgical Science,
Tokai University School of Medicine,
143 Shimokasuya, Isehara, Kanagawa, 259-1193, Japan
Telephone Number: +81 463 93 1121
FAX Number: +81 463 96 4404
E-mail: daisakai@is.icc.u-tokai.ac.jp

Introduction

Lower back pain is a common medical and social problem in the modern world. Therefore, there is an increasing interest in the development of new techniques for treating this problem. Since degeneration of the intervertebral disc is thought to have a close relationship with lower back pain, any strategy for delaying this degenerative process is of considerable clinical relevance (Gruber and Hanley, 1998; Phillips *et al.*, 2003).

Based on the fact that loss of cells and cell function in the nucleus pulposus is one of the most significant factors in disc degeneration, several studies have been reported with the aim of developing therapeutic techniques for this condition. These methods have included administration of bone morphogenetic protein-2 (BMP-2) and osteogenic protein-1 (OP-1; BMP-7) to increase the ability of disc cells to synthesize proteoglycans and collagen (Yoon *et al.*, 2003; Masuda *et al.*, 2003), transfer of the transforming growth factor-beta1 (TGF-β1) gene into nucleus cells using a viral vector (Nishida *et al.*, 1998), direct injection of collagen or a proteoglycan-like construct into the discs (Klein *et al.*, 2003), implantation of an artificial nucleus pulposus or disc (Mizuno *et al.*, 2004; Alini *et al.*, 2003) and implantation of mesenchymal stem cells into the discs (Sakai *et al.*, 2006).

Low-intensity pulsed ultrasound (LIPUS) has been shown clinically to be an effective noninvasive method for the stimulation of bioactivity (Duarte, 1983; Warden, 2000; Mayr *et al.*, 2000; Nolte *et al.*, 2001; Gebauer *et al.*, 2005). In an attempt to prevent disc degeneration and to find new techniques for maintaining disc function, we performed an experiment to determine whether LIPUS stimulation has any effect on the biological properties of disc cells, and found that LIPUS stimulation upregulates cell proliferation and proteoglycan (PG) synthesis in rabbit disc cells (Iwashina *et al.*, 2006). However, no study has yet confirmed the influence of LIPUS on human disc cells. The present study was therefore performed to verify whether LIPUS could stimulate disc cell proliferation and PG production in human nucleus pulposus cells using HNPSV-1, a cell line derived from human nucleus pulposus cells which maintains the original three-dimensional architecture of the cells and their gene expression profile (Sakai *et al.*, 2004). Furthermore, if LIPUS does upregulate cell proliferation and PG production in HNPSV-1 cells, changes in the expression of growth factor-related and matrix interaction-related genes were examined by cDNA microarray, in order to clarify the factors participating in LIPUS-induced

upregulation, while real-time PCR was used to quantify the changes in growth factor related gene expression.

Materials and Methods

Cell isolation and culture

The HNPSV-1 cells, cryopreserved in liquid nitrogen, were quickly thawed. The isolated cells were seeded in 6-well culture plates (Primaria, BD, Franklin Lakes, NJ, USA) at cell densities of 3.2×10^4cells/cm^2 in Dulbecco's modified Eagle medium (DMEM, Gibco; Life Technologies, Carlsbad, CA, USA) with 10% fetal bovine serum (FBS, Gibco), penicillin (100 μg/ml) and streptomycin (250 ng/ml) at 37°C, in a 5% CO_2 atmosphere.

Culture of HNPSV-1 cells in alginate

After three passages, the cultured cells were detached with trypsin-EDTA solution (0.05% trypsin, Gibco) and counted using a haemocytometer. The cells were collected by centrifugation and resuspended in 1.2% low-viscosity alginate (Clonetics; Lonza, Basel, Switzerland) in 0.15 M sodium chloride at a concentration of 1×10^5 cells/ml. The cell suspension was gently expressed through an 18-gauge needle attached to a 1-ml syringe into a 102 mM calcium chloride solution (Clonetics) to form drops of semisolid beads. After 10 min of polymerization, the beads were washed three times with normal saline, and then three more times with DMEM. Ten beads were placed in each well of a 6-well plate (non-treated, Iwaki, Japan) and then incubated in DMEM (4.5 ml/well) supplemented with 10% FBS and penicillin (100 μg/ml) and streptomycin (250 ng/ml) at 37°C, in a 5% CO_2 atmosphere.

Ultrasound stimulation

We upgraded SAFHS (Sonic Accelerated Fracture Healing System; Tejin Pharma Ltd, Tokyo, Japan) as a special US generator, and it was used to deliver an ultrasound (US) signal with a spatial and temporal average intensity of 7.5, 15, 30, 60, or 120 mW/cm^2. The frequency was 1.5 MHz with a 200-μs tone burst repeated at 1.0 kHz. Each 6-well plate of the LIPUS group was placed on an ultrasonic transducer (Iwabuchi *et al.*, 2005). The volume of culture medium in each well was reduced to 4 ml to avoid spillage. After the plate cover had been removed, an anti-reflection chamber was placed in each well while taking care to avoid intoducing air bubbles. It was confirmed that the alginate beads were not compressed by the chamber. Coupling gel (Sono Jelly, Toshiba, Tokyo, Japan) was dripped onto all the transducers, and the output was confirmed using an output checker. Then the culture plate and chamber unit were set on the transducer, and stimulation with LIPUS was started. For cell proliferation and PG production studies, the cells in the US group were stimulated for 20 min each day at a multiple range of intensity (7.5, 15, 30, 60, 120 mW/cm^2) for five or twelve days, starting on the third day after seeding in alginate. Later, to evaluate the effect of LIPUS on gene expression, the intensity of LIPUS was fixed at 30 mW/m^2, which was the level confirmed to provide the greatest production of proteoglycan. The control plates were handled in the same manner without LIPUS, i.e., the cover of each plate was removed, a chamber was placed in each well, and the plate was left to stand at room temperature for 60 min under the same conditions.

Measurement of DNA synthesis

DNA synthesis was examined by uptake of [^{3}H]-thymidine. At days 5 and 12 after the daily ultrasonic stimulation, the medium in each plate was changed to complete medium containing [^{3}H]-thymidine at a concentration of 2 μCi/ml. At 18 h after the start of the labelling, the beads were washed twice in PBS and added to sodium citrate solution (55 mM, in 90 mM NaCl). The beads were dissolved and the two compartments [cell-associated matrix (CM) and further removed matrix (FRM)] were separated by mild centrifugation at 100 x *g* for 10 min at 4°C. Then 10% trichloroacetic acid (TCA) was added to each fraction. The fractions were centrifuged (3000 rpm for 10 min), and the supernatant (TCA) was removed. This procedure was repeated 5 times, and TCA-insolvable material was collected and dried with 70% ethanol. The dry material was treated overnight with 1 ml of solvent (Solvable™; Packard, Meriden, CT, USA) at 45°C, and 10 ml of liquid scintillation cocktail (AtomlightTM; Packard) was added for counting of emissions (Beckman LS4800, Fullerton, CA, USA). Radioactivity [in disintegrations per minute (dpm)] was divided by the amount of DNA calculated using the Hoechst33258 dye method. All the isotope experiments were repeated more than two times.

Measurement of PG synthesis

Incorporation of [^{35}S]-sulphate was used to measure PG synthesis. At the indicated times, cultures were labelled by transfer to complete medium containing [^{35}S]-sulphate at a concentration of 40 μCi/ml for 18 h. Subsequent PBS washes, dissolution of alginate, TCA treatment, drying, and scintillation counting were carried out using the same procedure as those for [^{3}H]-thymidine uptake.

Measurement of DNA content

DNA content was measured using the fluorometric method as described previously. On days 0, 5 and 12 after US stimulation, beads in each well were collected and dissolved in sodium citrate solution (55 mM, in 90 mM NaCl) for 10 min at 4°C. After centrifugation, separated CM fractions were digested for 18 h at 55°C in papain solution (20 μg/ml in 50 mM EDTA, 5 mM L-cystein). Then 100 μl of Hoechst 33258 dye solution (1 μg/ml, pentahydrate, Molecular Probes, Eugene, OR, USA) was mixed with the digested sample, and 2 h later the emission spectrum of the mixture was determined for excitation at 365 nm by measuring the fluorescence emission of 460 nm using a plate reader (FL500, Bio-Tek, Highland Park, VT, USA). The standard curve was determined using known concentrations of calf thymus DNA (Sigma, St. Louis, MO, USA).

Measurement of PG content

PG content was measured by dimethylmethylene blue (DMMB, Polysciences, Warrington, PA, USA) assay. On days 5 and 12 after starting US, the beads were harvested,

dissolved, and the two matrix compartments, CM and FRM, were separated as described above. Each fraction was digested with papain (concentration of papain: CM; 20 μg/ml, FRM; 40 μg/ml) at 55°C for 18 h. The digested sample solution (75 μl) was mixed with 25 μl of 2.88 M GuHCl solution and 200 μl of DMMB reagent in a 96-well plate and immediately the absorbance at 530 nm and 595 nm was measured using a plate reader (SPECTRA MAX250, Molecular Devices, MDS, Toronto, Canada). Purified bovine nasal septum-D1 PG (Sigma) was used as a standard, and the 530 nm/595 nm ratio was calculated. The total amount of PG per well was normalized versus the total amount of DNA per well.

Harvesting of cells for RNA isolation

After completing the LIPUS treatment, 10% FBS was injected into each well twice to wash out the medium. Then the beads in each well were transferred to a conical tube with a spoon, stirred with 55 mM sodium citrate in 90M NaCl, and cooled to 4°C. The tube was centrifuged after 30 min to separate three layers, which comprised a white bottom layer and a middle layer composed of alginate beads with cells, as well as a top layer composed of alginate beads without cells. The top layer was discarded and then the same procedure was repeated to collect the cells in the beads.

SV Total RNA Isolation System

Total RNA was isolated using an SV Total RNA Isolation System (Promega R, Madison, WI, USA) according to the protocol provided by the manufacturer. An SV RNA lysis buffer was added to the harvested cells, and the mixture thus obtained was homogenized by repeated pipetting with a 20-gauge needle. The homogenate was mixed with SV RNA dilution buffer, centrifuged, and then heated at 70°C for 3 min. The supernatant thus obtained was collected, mixed with 95% ethanol, and centrifuged with a spin column to extract total RNA. After the RNA was isolated, genomic DNA was removed using DNAse (Qiagen, Venlo, The Netherlands).

Complementary DNA microarray

RNA extracted from the cells of the LIPUS group treated with 30 mW/m^2 of ultrasound for three days and from the cells of the control group was used to synthesize cDNA. The targets were prepared using the Atlas Glass Fluorescent Labelling Kit (Clontech Laboratories, Mountain View, CA, USA). This kit provides for indirect, "two-step" labelling of the target cDNA. Two-step labelling typically incorporates higher levels of label than direct, single-step procedures that directly incorporate fluorescently tagged nucleotides during cDNA synthesis. Target preparation began with 20 μg of total RNA. Aminoallyl-dUTP was incorporated during first-strand cDNA synthesis. Fluorescent dye (Cy3 or Cy5) was covalently coupled to aminoallyl-dUTP in the first-strand cDNA. The resulting labelled cDNA was purified using the Atlas NucleoSpin Extraction Kit (Clontech). The absorbance of each target was determined by optical density measurements at 260 nm (DNA) and either 550 nm (Cy3) or 650 nm (Cy5). The total dye content (pmoles), amount of probe (ng), and specific activity (number of Cy molecules incorporated/number of bases) was calculated for each target synthesized. The optimal incorporation of dye ranged from 20 to 50 covalently linked dye per 1000 nucleotides. Hybridization of the targets was performed using the Atlas™ Glass Array Human 1.0K Microarray (Clontech) technique to analyze the expression of 1101 spotted genes based on their fluorescence intensity. The slides were hybridized overnight at 50°C. Following hybridization, slides were washed, dried and then scanned using a ScanArray 5000XL laser scanner (PerkinElmer LAS, Inc., Shelton, CT, USA). The images were analyzed using QuantArray Microarray Analysis Software, Version 3.0 (Packard BioChip Technologies). Because the microarray analysis was performed in order to find factors upregulating cell proliferation and PG production, attention was focused on changes in expression of growth factor-related and matrix interaction-related genes.

Real-time PCR

Real-time PCR was performed to assess changes in expression quantitatively focusing on growth factor genes whose level of expression that showed differences of more than 1.5 fold mean signal ratio between the treated and control cultures in the above microarray analysis. Customized TaqMan probes for the designated genes whose 5'-3' ends were hybridized with a fluorescence-labelled oligonucleotide were purchased from Applied BioSystems (Carlsbad, CA, USA). In brief, cDNA was synthesized from total RNA. When the target DNA was annealed with specific oligonucleotide primers and TaqMan probes, hydrolysis occurred at the 5' end, followed by release of the dye, generating fluorescence. This fluorescence was used to detect and measure the expression of the genes. The sequences of the primers were obtained from the GeneBank database (National Center for Biotechnology Information Gene Bank database). Table 1 shows the sequences of the probes. ABI PRISM 7700™ Sequence Detector (Applied BioSystems) software was used for analysis, and a Gene Pix (Molecular Devices) scanner was used to measure fluorescence. The thermal cycler was set for the following conditions: 50°C for 1 min during Stage 1, 60°C for 30 min during Stage 2, and 95°C for 5 min during Stage 3. The number of cycles was set at 40. To provide an internal standard for correcting RNA purity, glyceraldehyde-3-phosphate dehydrogenase (GAPDH) was used as a housekeeping gene. Array Gauge diagnostic software (FujiFilm, Tokyo, Japan) was employed for analysis. This software automatically drew the amplification curve of each gene, which was combined with a threshold line to measure the threshold cycle of each gene. Then the comparative delta-delta Ct technique was used to quantify the relative initial concentration of each gene from the number of cycles required for amplification in relation to the logarithmic value of the initial concentration of the GAPDH standard.

Statistical analyses

All experiments were performed in triplicate. Results were expressed as mean ± standard deviation of three experiments. Significance of differences was assessed

using two-way analysis of variance (ANOVA) with Fisher's PLSD test as a *post hoc* test for cell proliferation and PG production analysis, with the level of significance set at $p<0.05$. For microarray analysis, the Mann-Whitney U test was chosen to evaluate the significance of differences in expression levels because of the size and distribution of the samples in this expression study. This non-parametric two-tailed test is not based on assumptions about the distribution of expression values (e.g., normal distribution) or the equality of variance. For all tests, differences at $p<0.05$ were considered significant.

Results

[^{3}H]-Thymidine incorporation

DNA synthesis, measured as the incorporation of [^{3}H]-thymidine (Fig. 1), was significantly increased in the 60 mW/cm^2 and 120 mW/cm^2 groups compared with the control group on Day 5 of ultrasound treatment (60 mW: 34.42 $\times 10^3$ dpm/μg DNA, p=0.0071; 120 mW: 33.10 $\times$ 10^3 dpm/μg DNA, p=0.0340). However, no significant difference was noted between the control and treated groups on Day 12.

Hoechst 33258 assay

A gradual increase of DNA through the 14-day culture period was confirmed in all of the groups (Fig. 2). There was a significant increase of DNA in the 120 mW/cm^2 group as compared with the control group on Days 5 and 12 of ultrasound treatment (5 days: 120 mW, 1.37 μg/well, p=0.0162; 12 days: 120 mW, 2.66 μg/well, p=0.0162). As observed with respect to the incorporation of [^{3}H]-thymidine (see above), there was a significant increase of DNA due to ultrasound treatment in the 120 mW/cm^2 group.

[^{35}S]-Sulphate incorporation

Synthesis of proteoglycans, measured as the incorporation of [^{35}S]-sulphate, was significantly increased on Day 14 compared with Day 7 (Fig. 3). Incorporation of [^{35}S]-sulphate was significantly increased in the 7.5, 15, 30, 60 and 120 mW/cm^2 groups compared with the control group on Days 5 and 12 of ultrasound (Fig. 3). In particular, the synthesis of proteoglycans was markedly increased in the 30 mW/cm^2 group compared with the other groups on both Days 5 and 12.

DMMB assay

Proteoglycans were quantified by the DMMB assay. The proteoglycan level increased as the culture period was prolonged (Fig. 4. It was significantly increased in the 15, 30, 60 and 120 mW/cm^2 groups compared with the control group on Day 5 of ultrasound treatment (Fig. 4). It was also significantly increased in the 7.5, 15, 30, 60 and 120 mW/cm^2 groups compared with the control group on Day 12 (Fig. 4). Although the proteoglycan level was increased in all of the treated groups, there were no significant differences between any of them.

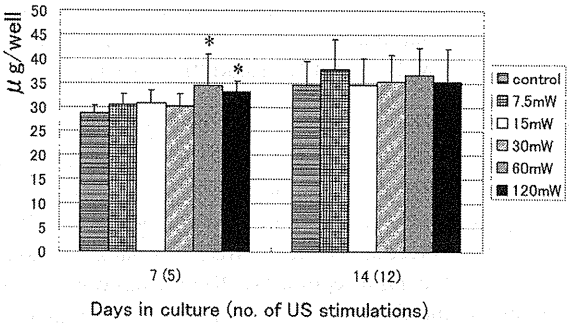

Figure 1. Cell proliferation rate is expressed as [^{3}H]-thymidine incorporation divided by DNA content per well. [^{3}H]-thymidine incorporation is significantly increased in the 60 and 120mW groups compared with the control group on Day 5 of LIPUS group.

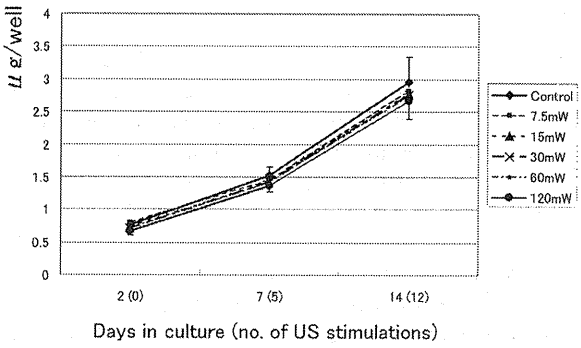

Figure 2. Cell number is represented as the DNA content per well. There was a gradual increase of DNA content through the 14-day culture period. On Day 5 and 12 after the start of ultrasound stimulation, there was a significant increase of DNA in the 120mW groups compared with the control group.

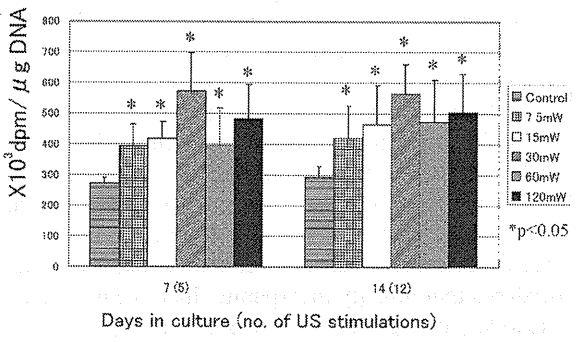

Figure 3. PG synthesis per DNA in control and LIPUS group cultures. PG synthesis is expressed as [S]-sulphate incorporation per culture over a period of 18h, divided by DNA content. PG synthesis significantly increased on Day 14 compared with Day 7. Regarding intensity of ultrasound, positive effect of PG synthesis was at its best at stimulation of 30mW.

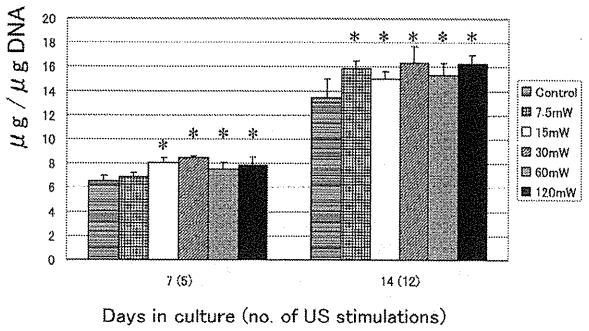

Figure 4. At 7 and 14 days of culture, PG content was measured by DMMB assay. On day 5 after the start of LIPUS stimulation, there was a significant increase in the 15, 30, 60 and 120mW group compared with the control group. On day 12 after the start of LIPUS stimulation, there was a significant increase in the 7.5, 15, 30, 60 and 120mW groups compared with the control group.

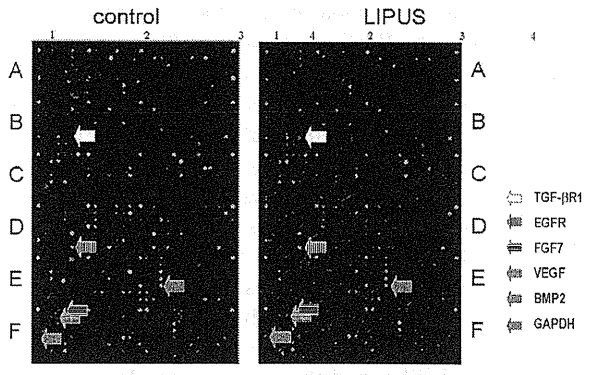

Figure 5. Gene pix showed higher signal intensity in growth factor expression in LIPUS group compared to control group.

Table 1. Microarray analysis results for growth factor and matrix related genes. Mean signal ratio in LIPUS treated group *versus* the control is indicated.

classification	Gene	mean ratio	
growth factor	transforming growth factor beta receptor type 1 (TGF-beta receptor type 1; TGFBR1; TGFR1)	4.76	↑↑
	Bone morphogenetic protein 2A (BMP2A)	1.93	↑↑
	fibroblast growth factor 7 (FGF7); keratinocyte growth factor (KGF)	1.82	↑↑
	epidermal growth factor receptor (EGF receptor; EGFR)	1.82	↑↑
	vascular endothelial growth factor (VEGF); vascular permeability factor (VPF)	1.55	↑↑
	Bone morphogenetic protein 7 (BMP7); osteogenic protein 1 (OP1)	1.46	↑
	growth differentiation factor 15 (GDF15)	1.45	↑
	fibroblast growth factor 8 (FGF8)	1.44	↑
	fibroblast growth factor 6 (FGF6)	1.35	↑
	transforming growth factor beta receptor III (TGF beta receptor III; TGFR3); betaglycan	1.34	↑
	Bone morphogenetic protein 8 (BMP8; osteogenic protein 2 (OP2)	1.28	↑
	insulin-like growth factor I receptor (IGF1R)	1.25	↑
	growth differentiation factor 1 (GDF1)	1.23	↑
	insulin-like growth factor I (IGF1); somatomedin C	1.23	↑
	fibroblast growth factor 3 (FGF3)	1.22	↑
	transforming growth factor beta (TGF-beta; TGFB)	1.00	↑
	Bone morphogenetic protein 5 (BMP5)	0.92	↓
	Bone morphogenetic protein 1 (BMP1)	0.85	↓
proteoglycan	Bone marrow proteoglycan 2	4.09	↑↑
	Bone proteoglycan II (PGS2); decorin (DCN)	2.01	↑↑
	Bonetcartilage small proteoglycan 1 (PGS1); biglycan (BGN)	1.03	↑
	heparan sulfate proteoglycan (HSPG2)	1.20	↑
collagen	collagen XVIII alpha 1 subunit (COL18A1)	2.71	↑↑
	collagen VI alpha 3 subunit (COL6A3)	2.33	↑↑
	collagen XI alpha 1 subunit (COL11A1)	2.31	↑↑
	procollagen IV alpha 2 subunit (COL4A2)	2.22	↑↑
	collagen IV alpha 6 subunit (COL4A6)	2.10	↑↑
	collagen IV alpha 3 subunit (COL4A3)	2.05	↑↑
	laminin beta 1 subunit (laminin B1; LAMB1)	1.49	↑
	collagen III alpha 1 subunit (COL3A1)	1.17	↑
	procollagen II alpha 1 subunit (COL2A1)	1.04	↑
	collagen VIII alpha 1 subunit (COL8A1)	0.98	↓
	laminin beta 2 subunit (laminin B2; LAMB2); S-laminin	0.94	↓
	collagen I alpha 2 subunit (COL1A2)	0.85	↓
	collagen VI alpha 2 subunit (COL6A2)	0.74	↓
	laminin gamma 1 subunit (LAMC1); laminin B2 subunit (LAMB2)	0.47	↓
MMP	matrix metalloproteinase 8 (MMP8); neutrophil collagenase (CLG1); PMNL collagenase (PMNL-CL)	2.82	↑↑
	matrix metalloproteinase 15 (MMP15); membrane-type matrix metalloproteinase 2 (MT-MMP2)	2.04	↑↑
	matrix metalloproteinase 9 (MMP9); gelatinase B; 92-kDa type IV collagenase (CLG4B)	1.87	↑
	matrix metalloproteinase 17 (MMP17); membrane-type matrix metalloproteinase 4 (MT-MMP4)	1.72	↑
	matrix metalloproteinase 3 (MMP3); stromelysin 1 (STMY1; SL1); transin 1	1.57	↑
	matrix metalloproteinase 16 (MMP16); membrane-type matrix metalloproteinase 3 (MT-MMP3); MMP-X2	1.32	↑
	matrix metalloproteinase 2 (MMP2); gelatinase A; 72-kDa type IV collagenase (CLG4A)	1.30	↑
	matrix metalloproteinase 1 (MMP1); interstitial collagenase (CLG); fibroblast collagenase	1.24	↑
	matrix metalloproteinase 13 (MMP13); collagenase 3 (CLG3)	1.02	↑
	matrix metalloproteinase 12 (MMP12); metalloelastase	0.62	↓
TIMP	tissue inhibitor of metalloproteinase 2 (TIMP2); CSC-21K	3.01	↑↑
	tissue inhibitor of metalloproteinase 1 (TIMP1); erythroid potentiating activity protein (EPA); collagenase inhibitor (CLGI)	2.49	↑↑
	tissue inhibitor of metalloproteinase 4 (TIMP4)	1.00	---

Table 2. Real-time PCR probe sequences and fluorescence intensities of the amplified genes

Gene	**Sequence (5'-3')**	**Intensity**
GAPDH	GGGCGCCTGGTCACCAGGGCTGCTT	1.000
BMP2	TTCCACCATGAAGAATCTTTGGAAG	1.975 (p=0.013)
TGF-βR1	CAGGTTCTGGCTCAGGTTTACCATT	1.643 (p=0.013)
FGF7	TCTATGCAAAGAAAGAATGCAATGA	1.345 (p=0.002)
EGFR	GAGCGAAGTTTTATGCAAGGGTAAC	1.628 (p=0.002)
VEGF	CACCATGCCAAGTGGTCCCAGGCTG	1.532 (p=0.034)

Oligonucleotide primers and Taq man probes were designed based on sequences from the Gene Bank database.

Microarray analysis

Analysis of 1101 genes showed that the expression of 846 genes in the LIPUS group was increased in comparison with the control group. Among these 846 genes, 114 (spot intensity >70 x control) had fluorescence intensity above the threshold value, and these included genes relating to growth factors and matrix interaction, such as TGF-β receptor type 1 (TGF-β R1), BMP2, fibroblast growth factor 7 (FGF7), endothelial growth factor (EGFR), and vascular endothelial growth factor (VEGF). An increase of expression was also observed for the heparan sulphate and biglycan genes, whose products are extracellular matrix components, as well as the type IV and VI collagen genes. Among the genes with increased expression, genes categorized in growth factors that had the mean signal difference of greater than 1.5 fold in LIPUS treated group were compared. As a result, it was confirmed that the fluorescence intensity of the BMP2, TGF-β R1, FGF7, EGFR, and VEGF genes was significantly increased in the LIPUS group compared with the control group (Fig. 5; Table 1).

Real-time PCR

Results of real-time PCR confirmed quantitatively that there were significant changes in the expression of the TGF-β R1, BMP2, FGF7, EGFR, and VEGF genes after LIPUS stimulation. RNA was extracted in order to synthesize cDNA, and the fluorescence intensities of the amplified genes measured with TaqMan probes are given in Table 2.

Discussion

The use of LIPUS to noninvasively increase bioactivity is now widely applied to the treatment of fractures with non-union. LIPUS has been reported to increase the ability of cartilage cells to synthesize proteoglycans and to promote aggrecan gene expression (Paravizi *et al.*, 1999; Zhang *et al.*, 2002). It has also been reported that Ca^{2+} signalling is required to increase the synthesis of aggrecan (Paravizi *et al.*, 2002). Further, the ability of cartilage cells to synthesize type II collagen is increased and the expression of type X collagen is inhibited when cartilage cells in three-dimensional culture (alginate bead encapsulation) are treated with LIPUS (Zhang *et al.*, 2003). Since it has often been reported that apoptosis and reduced function of cells in the nucleus pulposus may trigger intervertebral disc degeneration, and it is clinically important to maintain or to upregulate the biological activity of nucleus pulposus cells, we treated nucleus pulposus cells with LIPUS to examine its potential as a noninvasive therapy for preserving the original structure and function of the intervertebral discs. The present experiment was designed to determine whether LIPUS increased the bioactivity of human nucleus pulposus cells and to examine the optimum conditions for performing LIPUS and the factors involved in activation of the cells at the gene level using the HNPSV-1 cell line established from normal human nucleus pulposus cells.

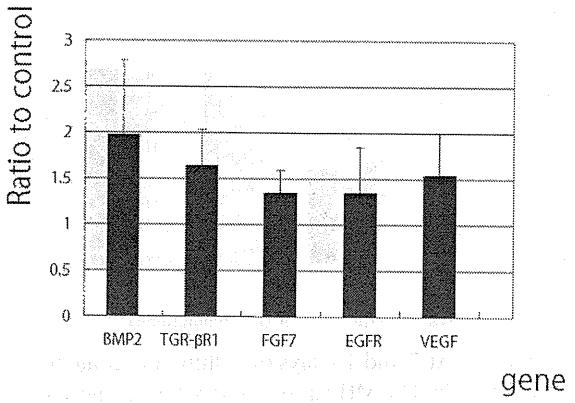

Figure 6. Real time RT-PCR results confirmed upregulation of multiple growth factors in the LIPUS group compared to control group.

There have been several reports that LIPUS stimulates rabbit and bovine nucleus pulposus cells to synthesize proteoglycans (Miyamoto *et al.*, 2005; Iwashina *et al.*, 2006). Although LIPUS has a positive effect in animals, it is necessary to perform experiments on human nucleus pulposus cells before clinical application can be considered. A massive number of cells would be required to examine the optimum conditions for LIPUS. However, it is difficult to obtain the necessary number of normal human nucleus pulposus cells for such experiments because it is difficult to obtain nucleus pulposus tissue during surgery, and such tissue is often damaged. Therefore, the HNPSV-1 clone obtained by immortalizing normal human nucleus pulposus cells was used to examine the effect of LIPUS and the optimum conditions for its use. Since HNPSV-1 cells resemble normal human nucleus pulposus cells with respect to gene expression and matrix synthesis, use of this cell line should provide results comparable to those obtained by treating actual human nucleus pulposus cells with LIPUS.

The results of the present study showed that cell growth, as measured by [^{3}H]-thymidine incorporation, was increased in the 60 and 120 mW/cm^2 groups on Day 5, although the DNA content was increased only in the 120 mW/cm^2 group. This may have been due to the fact that culture in alginate was more suitable for matrix synthesis than cell growth in monolayer culture. Another possible reason may have been that the proliferative activity of HNPSV-1 was already fully stimulated, in view of the original report by Sakai *et al.* (2004) indicating that the growth rate of HNPSV-1 cells was more than six times faster than that of normal cells.

The synthesis of proteoglycans was significantly increased in all of the treated groups compared with the control group, and the increase was particularly marked in the 30 mW/cm^2 group. Similarly, the DMMB assay showed that the amount of proteoglycan synthesized was significantly increased in the 15, 30, 60 and 120 mW/cm^2 groups on Day 5 and in all of the treated groups on Day 7, relative to the control group. Accordingly, LIPUS may significantly increase the ability of human nucleus

pulposus cells to synthesize proteoglycans and also augment the amount of proteoglycan synthesized by these cells. A previous experiment using cartilage cells in three-dimensional culture showed that LIPUS did not alter cell growth, but increased proteoglycan synthesis at 50 or 120 mW/cm^2 (Iwashina *et al.*, 2006). The present study showed that LIPUS stimulated the synthesis of proteoglycans, which are important matrix components for nucleus pulposus cells, consistent with earlier data for other cell types.

It is thought that LIPUS vibrates the extracellular matrix and thus subtly alters the pericellular environment, thereby stimulating various receptors and adhesion factors on the cell surface. A previous report that stimulation of human fibroblasts with LIPUS activated a cell adhesion factor also supports the present finding that LIPUS increased the capacity of HNPSV-1 cells to synthesize proteoglycans and also increased the amount synthesized (Zhou *et al.*, 2004).

Iwashina *et al.* (2006) performed a similar study in which intervertebral disc cells from rabbits were treated with LIPUS. They showed that the proliferative activity of nucleus pulposus cells was increased only at a low intensity, and that there was no significant difference of proteoglycan synthesis between the treated and control groups during the early stage of exposure to ultrasound. In the present experiment with a human cell line, growth was increased only at high levels of ultrasound intensity, but proteoglycan synthesis was significantly increased at all intensity levels from the early stage of treatment. Since rabbit nucleus pulposus cells are heterogeneous and include many cells derived from the immature notochord, they show individual variation that tends to minimize any difference from the control group. In contrast, HNPSV-1 cells are a monoclonal cell line, and thus may respond uniformly to LIPUS.

Since it remains unknown how LIPUS stimulates the capacity of nucleus pulposus cells to synthesize proteoglycans, we investigated the mechanism responsible by the microarray technique. We found an increase in the expression of genes for small proteoglycans such as heparan sulphate and biglycan, as well as genes for growth factors that enhance disc cell activity, such as TGF-β R1, BMP2,0FGF7, EGFR. VEGF was also found to be increased, and this has recently been reported to play a role in nucleus pulposus cell survival (Fujita *et al.*, 2008). As growth factors like BMP2 and TGF-β1 have already been reported to increase the synthesis of proteoglycans by nucleus pulposus cells (Yoon *et al.*, 2003), the increased expression of such factors and their receptors suggests involvement of these genes in the increased bioactivity of nucleus pulposus cells after LIPUS stimulation.

We have not examined the effect of timing on when to apply LIPUS in this experimental series due to limited sample size. The timing factor as well as the LIPUS intensity may produce different effects.

Several studies have already investigated therapeutic techniques for increasing the activity of disc cells. Although LIPUS alone failed to provide a sufficient therapeutic effect, the present results suggest that this treatment is still worth considering for enhancement of growth factor expression, and that it in combination with other cell-stimulating techniques, merits further research. Furthermore, since there are limitations for an *in vitro* experiment, it is to be noted that the effect may not be as effective *in vivo*.

Conclusions

The present study has demonstrated that LIPUS treatment stimulates cell proliferation and production of proteoglycan in human nucleus pulposus cell line, possibly by enhancement of growth factor-related genes. Although the current experiment was based on *in vitro* research, LIPUS may be a clinically effective therapeutic technique because it is non-invasive, and can be combined with recently developed therapeutic methods to inhibit disc degeneration, possibly producing a synergistic effect.

Acknowledgements

This work was supported in part by Grant-in-Aid for Scientific Research (grant numbers 16390443, 18791060), a Grant of The Science Frontier Program from the Ministry of Education, Culture, Sports, Science and Technology of Japan, a grant from 2007 Tokai University School of Medicine Research Aid, and from AO Spine International.

References

Alini M, Li W, Markovic P, Aebi, M, Spiro R, Roughley P (2003) The potential and limitations of a cell-seeded collagen/hyaluronan scaffold to engineer an intervertebral disc-like matrix0Spine **28**: 973-981.

Duarte LR (1983) The stimulation of bone growth by ultrasound. Arch Orthop Trauma Surg **101**: 153-159.

Fujita N, Imai J, Suzuki T, Yamada M, Ninomiya K, Iwasaki R, Morioka H, Matsumoto M, Chiba K, Watanabe S, Suda T, Toyama Y, Miyamoto T (2008) Vascular endothelial growth factor-A is a survival factor for nucleus pulposus cells in the intervertebral disc. Biochem Biophys Res Commun **372**: 367-372.

Gebauer D, Mayr E, Orthner E, Ryaby JP (2005) Low-intensity pulsed ultrasound: Effects on nonunions. Ultrasound in Med Biol **31**: 1391-1402.

Gruber HE, Hanley Jr EN (1998) Analysis of aging and degeneration of the human intervertebral disc. Comparison of surgical specimens with normal controls. Spine **23**: 751-757.

Iwabuchi S, Ito M, Hata J, Chikanishi T, Azuma Y, Haro H (2005) *In vitro* evaluation of low-intensity pulsed ultrasound in herniated disc resorption. Biomaterials **26**: 7104-7114.

Iwashina T, Mochida J, Miyazaki T, Watanabe T, Iwabuchi S, Ando K, Hotta T, Sakai D (2006) Low-intensity pulsed ultrasound stimulates cell proliferation and proteoglycan production in rabbit intervertebral disc cells cultured in alginate. Biomaterials **27**: 354-361.

Klein RG, Eek BC, O'Neill CW, Elin C, Mooney V, Derby RR (2003) Biochemical injection treatment for discogenic low back pain: a pilot study. Spine J **3**: 220-226.

Masuda K, Takegami K, An H, Kumano F, Chiba K, Andersson GB, Schmid T, Thonar E (2003) Recombinant osteogenic protein-1 upregulates extracellular matrix metabolism by rabbit annulus fibrosus and nucleus pulposus cells cultured in alginate beads. J Orthop Res **21**: 922-930.

Mayr E, Frankel V, Ruter A (2000) Ultrasound-An alternative healing method for nonunions? Arch Orthop Trauma **120**: 1-8.

Miyamoto K, An HS, Sah RL, Akeda K, Okuma M, Otten L, Thonar EJ, Masuda K (2005) Exposure to pulsed low intensity ultrasound stimulates extracellular matrix metabolism of bovine intervertebral disc cells cultured in alginate beads. Spine **30**: 2398-2405.

Mizuno H, Roy AK, Vacanti CA, Kojima K, Ueda M, Bonassar LJ (2004) Tissue-engineered composites of annulus fibrosus and nucleus pulposus for intervertebral disc replacement. Spine **29**: 1290-1297.

Nishida K, Kang JD, Suh JK, Robbins PD, Evans CH, Gilbertson LG (1998) Adenovirus-mediated gene transfer to nucleus pulposus cells: implication for the treatment of intervertebral disc degeneration. Spine **23**: 2437-2443.

Nolte PA, Krans A, Patka P, Janssen IMC, Ryaby JP, Albers GHR (2001) Low-intensity pulsed in the treatment of nonunions. J Trauma **51**: 693-702.

Paravizi J, Wu CC, Lewallen DG, Greenleaf JF, Bolander ME (1999) Low-intensity ultrasound stimulates proteoglycan synthesis in rat chondrocytes by increasing aggrecan gene expression. J Orthop Res **17**: 488-494.

Paravizi J, Parpura V, Greenleaf JF, Bolander ME (2002) Calcium signaling is required for ultrasound stimulated aggrecan synthesis by rat chondrocytes. J Orthop Res **20**: 51-57.

Phillips FM, An H, Kang JD, Boden SD, Weinstein J (2003) Biologic treatment for intervertebral disc degeneration. Spine **28**: S99.

Sakai D, Mochida J, Yamamoto Y, Toh E, Iwashina T, Miyazaki T, Inokuchi S, Ando K, Hotta T (2004) Immortalization of human nucleus pulposus cells by a recombinant SV40 adenovirus vector: establishment of a novel cell line for the study of human nucleus pulposus cells. Spine **29**: 1515-1523.

Sakai D, Mochida J, Iwashina T, Hiyama A, Omi H, Imai M, Nakai T, Ando K, Hotta T (2006) Regenerative effects of transplanting mesenchymal stem cells embedded in atelocollagen to the degenerated intervertebral disc. Biomaterials **27**: 335-345.

Warden SJ, Bennell JM, McMeeken JM, Wark JD (2000) Acceleration of fresh fracture repair using the sonic accelerated fracture healing system (SAFUS): A review. Calcif Tissue Int **66**: 157-163.

Yoon ST, Su Kim K, Li J, Soo Park J, Akamaru T, Elmer WA, Hutton WC (2003) The effect of bone morphogenetic protein-2 on rat intervertebral disc cells in vitro. Spine **28**: 1773-1780.

Zhang ZJ, Huckle J, Francomano CA, Spencer RG (2002) The influence of pulsed low-intensity ultrasound on matrix production of chondrocytes at different stages of differentiation: an explant study. Ultrasound Med Biol **28**: 1547-1553.

Zhang ZJ, Huckle J, Francomano CA, Spencer RG (2003) The effects of pulsed low intensity ultrasound on chondrocyte viability, proliferation, gene expression and matrix production. Ultrasound Med Biol **29**: 1645-1651.

Zhou S, Schmelz A, Seufferlein T, Li Y, Zhao J, Bachem MG (2004) Molecular mechanisms of low intensity pulsed ultrasound in human skin fibroblasts. J Biol Chem **24**: 54463-54469.

Discussion with Reviewer

S. Ferguson: Gene expression rates were quantified by means of real-time PCR results. However, many of the genes which were considered significantly up-regulated had mean ratios of less than two. Generally, unless the authors can demonstrate extremely tight control of their PCR process, it is accepted practice to require at least a two-fold increase in gene expression before considering a difference significant.

Authors: Protocol and efficiency level of real-time PCR in this experiment has been set with appropriate controls, tight cycle condition and repeated measures. Therefore, we believe that the results are valid to determine significance.

SPINE Volume 34, Number 14, pp 1448–1456

Differential Phenotype of Intervertebral Disc Cells

Microarray and Immunohistochemical Analysis of Canine Nucleus Pulposus and Anulus Fibrosus

Daisuke Sakai, MD, PhD,* Tomoko Nakai, BSc,* Joji Mochida, MD, PhD,* Mauro Alini, PhD,† and Sibylle Grad, PhD†

Study Design. Microarray gene expression profiling, quantitative gene expression analysis, and immunohistochemistry was used to investigate molecular variations between nucleus pulposus (NP) and anulus fibrosus (AF) of the dog intervertebral disc (IVD).

Objective. To identify specific molecules with differing expression patterns in NP and AF and compare their profile with articular cartilage (AC).

Summary of Background Data. Although experimental and animal studies have demonstrated the potential of cell based approaches for NP regeneration, there is still a deficiency of basic knowledge about the phenotype of IVD cells.

Methods. Comparative microarray analysis of beagle lumbar NP and AF was performed. Molecules of interest were evaluated by quantitative reverse transcriptase-polymerase chain reaction and immunohistochemistry, comparing lumbar and coccygeal NP and AF and AC. To assess interspecies variations, genes that had been found differentially expressed in rat tissues were also investigated.

Results. Forty-five genes with NP/AF signal log ratio ≥1 were identified. α-2-Macroglobulin, cytokeratin-18, and neural cell adhesion molecule (CD56) mRNA were higher in NP compared to AF and AC, and desmocollin-2 mRNA was higher in NP than AF. The expression profiles were similar in lumbar and coccygeal discs, although certain variations were noticed. Interspecies differences between rat and dog were evident in the expression of several genes. Immunohistochemistry confirmed differences in gene expression at the protein level.

Conclusion. This study reports on the expression of molecules that have not been described previously in IVD, in non-notochordal discs comparable with human. Interspecies differences were noted between rat and dog tissues, whereas variations between caudal and lumbar discs were less prominent. The NP of the beagle as a chondrodystrophoid dog breed is potentially more similar to the human than the NP of species whose discs do not naturally degenerate. Therefore, studies on appropriate species may contribute to a better understanding of the cell types residing in the IVD.

From the *Department of Orthopaedic Surgery, Surgical Science, Tokai University School of Medicine, Isehara, Kanagawa, Japan; and †Biomaterials and Tissue Engineering Program, AO Research Institute, Davos, Switzerland.

Acknowledgment date: August 5, 2008. First revision date: October 8, 2008. Acceptance date: January 19, 2009.

The manuscript submitted does not contain information about medical device(s)/drug(s).

No funds were received in support of this work. No benefits in any form have been or will be received from a commercial party related directly or indirectly to the subject of this manuscript.

Address correspondence and reprint requests to Sibylle Grad, PhD, AO Research Institute, Clavadelerstrasse 8, CH 7270 Davos, Switzerland; E-mail: sibylle.grad@aofoundation.org

Key words: Microarray, gene expression, immunolocalization, nucleus pulposus, anulus fibrosus, canine, chondrodystrophoid. **Spine 2009;34:1448–1456**

Intervertebral disc (IVD) degeneration, although in many cases asymptomatic, is associated with low back pain and diseases such as sciatica, disc herniation, or prolapse.[1,2] It implies a decrease in disc height and alterations in the mechanics of the spinal column, and in the long term it can lead to spinal stenosis, a major cause of pain and disability, especially in the elderly. The incidence of IVD degeneration is increasing exponentially, and it is increasingly recognized as a disorder that also affects the younger population. In fact, about 20% of people in their teens have discs with mild signs of degeneration.[3,4]

In view of the fact that current treatment methods may reduce pain but cannot repair the degenerated disc, there is an increasing interest in novel cell-based therapies. Their aim is to achieve cellular repair of the degenerated disc matrix to ultimately restore disc height and biomechanical function. One approach has been to stimulate the disc cells to increase the rate of matrix synthesis by application of growth factors or gene therapy.[5–8] However, because cell densities in human discs are low and their vitality in degenerate discs is impaired, stimulation of the remaining cells may be insufficient.[9] Cell implantation may overcome the paucity of cells in a degenerate disc. For cell therapy, mesenchymal stem cells have been proposed, and clinical procedures have been developed to inject these cells into a degenerated disc.[10–12] It has also been suggested that, similar to chondrogenic differentiation, mesenchymal stem cells can differentiate toward the NP cell phenotype *in vitro*.[13–15]

Although experimental work and animal studies have demonstrated the potential of cell-based approaches, there is still a deficiency of basic knowledge about the cellular components residing in the IVD. In a healthy disc, the cells of the nucleus pulposus (NP) function to maintain its highly hydrated gelatinous matrix, which is rich in proteoglycans and in collagen and elastin fibers. The NP is surrounded by the anulus fibrosus (AF), which is composed of a series of concentric lamellae, consisting of collagen and elastin fibers. Whereas the cells of the outer AF appear fibroblast-like and elongated, the NP cells in human adults are described as chondrocyte-like because of their

rounded morphology and their phenotypic profile. The NP and AF cells are generally referred to as IVD cells or chondrocytes, although they markedly differ from each other and from articular cartilage cells. Appropriate molecular markers that define NP and AF cells and differ from chondrocyte markers would be instrumental in evaluating and monitoring a cell population with respect to the IVD-like phenotype.

In a previous study, we reported a number of genes that were differentially expressed in NP, AF, and AC cells in rats.[16] Although distinct animal models are useful to investigate specific associations, considerable variations between species are evident, and findings cannot be translated from one to another species without careful consideration.[17] The present study used discs from dog of a chondrodystrophoid breed and microarray, quantitative reverse transcriptase-polymerase chain reaction (RT-PCR) and immunohistochemistry to identify potential new molecules with varying expression in NP and AF. Furthermore, because caudal discs are often used as models to study IVD biology and biomechanics, potential differences between caudal and lumbar discs were assessed with respect to the molecules of interest. Finally, the expression of the genes that had been found differentially expressed in the rat was also analyzed in the dog tissues. This allowed evaluating interspecies differences and similarities between animals with notochordal *versus* chondrocytic nucleus, which is of fundamental importance for the selection of a particular animal model to study IVD degeneration and regeneration.[17]

Materials and Methods

Microarray Analysis

All animal experiments were carried out according to the protocol approved by the Animal Experimentation committee at our institution (experiment #042015). Mature female beagle dogs (16–18 months old; n = 3; mean weight approximately 10 kg; Nosan Beagle, Nosan Corp., Kanagawa, Japan) were used for tissue harvest for microarray analysis. NP and AF were harvested from lumbar (L2–L3 to L5–L6) and caudal (C1/2 to C4/5) discs in an aseptic environment. Tissue samples were immediately placed in RNA*later* (Ambion, Austin, TX) and sent for microarray analysis service to Kurabo Industries Inc., Biomedical Dept., Osaka, Japan. This service included high-quality total RNA isolation, cDNA synthesis, biotin-labeled cRNA synthesis, cohybridization (NP/AF) to the Affymetrix GeneChip Dog Genome Array (Affymetrix Inc., Santa Clara, CA), array imaging, and analysis according to the protocol provided by the manufacturer (Affymetrix GeneChip Expression Analysis Technical Manual).[18,19] A total of 3 microarrays were prepared: NP/AF cohybridizations, each with dye-swap to exclude dye bias. The relative expression of each gene in NP *versus* AF was expressed as a ratio of fluorescence intensities.

Real-time RT-PCR

NP and AF were dissected from the lumbar (n = 9) and coccygeal (n = 4) discs as specified above. Articular cartilage was harvested from femoral condyles (n = 9) of the same animals.

Chopped tissue samples were placed in Isogen (Nippon Gene, Toyama, Japan), frozen in liquid nitrogen, and homogenized with a Polytron homogenizer. Total RNA was extracted by a modified TRISpin method,[20] using the SV Total RNA Isolation System (Promega, Madison, WI). Reverse transcription was performed with TaqMan reverse transcription reagents (Applied Biosystems, Foster City, CA) and random hexamer primers.

For real-time PCR, 5 genes were selected that showed a high signal ratio in the NP *versus* AF microarray comparison: α-2-macroglobulin (A2M), annexin A4 (ANXA4), desmocollin 2 (DSC2), cytokeratin 18 (CK18), and neural cell adhesion molecule 1 (NCAM1, CD56 140-kDa isoform). In addition, 5 genes, that had been found differently expressed in NP *versus* AC in the rat, were evaluated[16]: Cartilage oligomeric matrix protein (COMP), glypican 3 (GPC3), matrix Gla protein (MGP), pleiotrophin (PTN), and vimentin (VIM). Dog primers (Invitrogen, Carlsbad, CA) and TaqMan probes (Sigma, St. Louis, MO) were designed using Primer Express software, version 3.0 (Applied Biosystems) (Table 1). The assay for amplification of 18S ribosomal RNA was from Applied Biosystems. PCR was performed on a 7300 Real-Time PCR System (Applied Biosystems) with TaqMan Universal PCR Master Mix (Applied Biosystems), 900 nmol/L primers (forward and reverse), and 250 nmol/L TaqMan probe. Relative quantification of target mRNA was performed according to the comparative C_T method (ABI PRISM User Bulletin 2, Applied Biosystems) with 18S ribosomal RNA as the endogenous control. Gene expression levels of lumbar and coccygeal NP and AF were normalized to the values of their corresponding AC.

Statistical significance was determined with SPSS 14.0 software, using Kruskal-Wallis nonparametric analysis with Mann-Whitney *U post hoc* testing, and $P < 0.05$ was defined as significant.

Immunohistochemistry

Mouse anti-CD56 (NCAM1) (Clone 123C3) was purchased from Spring Bioscience (Montigny le Bretonneux, FR) and applied in the dilution 1:50; Rabbit anti-alpha 2 macroglobulin from GeneTex, Inc. (San Antonio, TX) was applied in the dilution 1:50; Rabbit anti-desmocollin 2 from Progen Biotechnik (Heidelberg, Germany) was applied in the dilution 1:50; Rabbit anti-glypican 3 (aa 303–464) from Santa Cruz Biotechnology (Santa Cruz, CA) was applied in the dilution 1:25; Mouse anti-cytokeratin 18 (Clone C-04) from Novus Biologicals, Inc. (Littleton, CO) was applied in the dilution 1:50.

Lumbar IVD, coccygeal IVD, and AC from the femoral condyle were harvested from 12-month-old female beagle dogs and fixed in 4% paraformaldehyde. Tissues were decalcified, embedded in paraffin, and cut into 3–5 μm sagittal sections. Sections were incubated with 0.005% proteinase (Sigma) at 37°C for 10 minutes and probed with relevant primary antibodies at 4°C for 16 hours. Subsequently, they were treated with appropriate biotinylated secondary antibodies at room temperature for 1 hour. Slides were then processed using Vectastain ABC Kit (Vector Laboratories), developed with 3,3′-diaminobenzidine (DAB) substrate and counterstained with hematoxylin.

For detection of CK18, tissues were embedded in OCT compound and cryosectioned into 6-μm-thick sections. IVD tissues were not decalcified and sectioned axially. Cryosections were incubated with primary antibody at 4°C for 16

Table 1. Oligonucleotide Primers and Probes Used for Real-Time PCR

Gene Name	Gene Symbol	Ref. Sequence	Primer Fw (5′-3′)	Primer Rev (5′-3′)	Probe (5′-FAM; 3′-TAMRA)
α-2-Macroglobulin	A2M	XM_534893	ACT TGG CTC ACT GCC TTT GTA CT	GTT GAG CAG AGA CCC GGA ACT	AGC ACA CAT CAC CCA AGC CCT CAT G
Annexin A4	ANXA4	NM_001003039	CCC AGC GCC AGG AGA TTA G	CGA CTT CAG GTC GTC CAT CA	ACG GCC TAC AAG AGC ACC ATC GGC
Cartilage oligomeric matrix protein	COMP	XM_533869	GCC GAG ACA CGG ATT TGG	CAC GTC CTC TTG CCC TGA GT	TTC CCC GAC GAG AAG CTC CGC
Desmocollin 2	DSC2	XM_537291	ACG ATG CAC ACA CGT CTC AAA	TGG TGA TCA CGC CTG TAG TTG	CCA TCA TCG AGC AGT TGC CAG CGT A
Glypican 3	GPC3	XM_538178	CAG CCT CTT TCC AGT CAT CTA CAC	CCC CTC GGA GGC ACT CAT	AGC TCA TGA ACC CCG GCC TGC
Cytokeratin 18	CK18	XM_849849	AAG AAC CAC GAG GAG GAA GTA AAG	CCC GGA TAT CTG CCA TGA TC	TCT ACA AAA CCA AAT CGC CAA CTC TGG G
Matrix Gla protein	MGP	XM_848662	CCA CCA AGC CCG CCT AT	GCG TAG CGT TCG CAA AGC	CTC AAC CGG GAA GCC TGT GAT GAC TTC
Neural cell adhesion molecule 1 (CD56 140-kDa isoform)	NCAM1	NM_001010950	AAG ACT CTG GAC GGG CAC AT	GGC GTC TGT GTA CTG GAT GCT	TGC GTA GCC ATG CCC GCG
Pleiotrophin	PTN	XM_532732	GTG CAG CAG CGT CGA AAA	TGT CCA CAG CTG CCA AGA TG	TGC AGC TGC CTT CCT GGC ATT CAT
Vimentin	VIM	XM_844468	CAG GCG AAG CAG GAG TCA AC	TCC CTT TGA GTG CAT CCA CTT	CCG GAG CCA GGT GCA GTC CCT C

Probes were labeled with the reporter dye molecule FAM (6-carboxyfluorescein) at the 5′ end and with the quencher dye TAMRA (6-carboxy-N, N, N′, N′-tetramethylrhodamine) at the 3′ end.

hours. Subsequently, sections were treated with anti-mouse Alexa Fluor 488 goat secondary antibody (1:200, Molecular Probes, Invitrogen). Nuclei were counterstained with 4′,6-diamidino-2-phenylindole (DAPI) and slides observed with fluorescence microscopy.

Results

Microarray

A comparative microarray analysis using the Affymetrix GeneChip Dog Genome Array, which are high-density oligonucleotide arrays (11-μm spots) containing 2,383,625-mer probe-sets detecting 21,700 transcripts was performed to identify genes that may be used to uniquely distinguish NP from AF cells. As we were particularly interested in potential NP marker molecules, the focus was laid on molecules with a high NP *versus* AF expression ratio. While examining the signal ratios in the NP *versus* AF microarray comparison, 45 genes with a signal log ratio of at least 1 were noted (Table 2). Furthermore, 77 genes had a signal log ratio of −1 or lower, 43 of which showed a ratio of −3 or lower (Table 3).

Eight genes were identified with an NP to AF signal log ratio higher than 3: Wnt inhibitory factor-1, CK18, A2M, desmoplakin, DSC2, UDP-glucose dehydrogenase, carbonic anhydrase II, and ADAMTS10. Among these genes, CK18, A2M, and DSC2 were selected for quantitative analysis by real-time RT-PCR, as they appeared valuable candidate genes for the characterization of NP cells. In addition, 2 genes with a signal log ratio of 1.4, namely, ANXA4 and NCAM1 (CD56), were further investigated.

Real-Time PCR

Data from lumbar discs are illustrated in Figure 1. In correlation with the microarray results, A2M, DSC2, CK18, and NCAM1 (CD56) mRNA levels were higher in NP compared to AF. The NP gene expression of A2M, CK18, and NCAM1 (CD56) was also enhanced when compared to AC, whereas no difference was noted in DSC2 gene expression between NP and AC. No differences in ANXA4 mRNA expression levels were found between NP, AF, and AC.

In contrast to previous findings in the rat, the GPC3 mRNA expression was equally low in NP as in AC. Hence, GPC3 expression was downregulated in the dog compared to the rat NP, while its expression was higher in dog AF than AC, which is similar to the rat results. The COMP, MGP, and VIM expression levels were lower in NP than in AF and AC, whereas PTN was lower in NP compared to AC. Additionally, MGP, PTN, and VIM mRNA values were lower in AF compared to AC.

Results from the coccygeal discs are illustrated in Figure 2, with data from the corresponding lumbar NP and AF shown for comparison. Essentially, the expression profile of the genes analyzed was similar in lumbar and coccygeal discs, showing stronger expression of A2M, CK18, and NCAM1 (CD56) in NP compared with AF and AC and higher DSC2 expression in NP than AF. In addition, GPC3 expression was significantly higher in coccygeal AF than NP. The mRNA expression of COMP, MGP, and PTN also demonstrated a similar pattern in coccygeal as in lumbar disc, showing lower expression levels in NP as compared to AC and higher AF than NP levels of COMP mRNA.

Variations between coccygeal and lumbar disc were noticed for NCAM1 (CD56), which was expressed more highly in coccygeal than in lumbar NP, and for PTN and VIM, which were expressed more highly in

Table 2. Genes With a Signal Log Ratio of 1 or Higher in the NP *Versus* AF Microarray Comparison

Signal Log Ratio	Signal Log Ratio Low	Signal Log Ratio High	Change in *P*	Representative Public ID	Gene Title	Gene Symbol
5.2	4.9	5.5	0.00002	CO629970	Similar to WIF-1	LOC481148
4.5	3.3	5.8	0.00006	CO673880	Similar to Keratin, type I cytoskeletal 18 (Cytokeratin 18) (K18) (CK 18)	LOC477601
3.7	3.3	4	0.00002	CO664742	Similar to alpha 2 macroglobulin	LOC477699
3.5	2.8	4.1	0.00002	CO704199	Similar to Desmoplakin (250/210 kDa paraneoplastic pemphigus antigen)	LOC488207
3.4	2.2	4.6	0.000023	CO614128	Desmocollin type 2	DSC2
3.4	1.5	5.2	0.000618	CO678462	Similar to UDP-glucose dehydrogenase	LOC479106
3.3	3	3.5	0.00002	CF409351	Similar to carbonic anhydrase II (carbonate dehydratase II) (CA-II) (carbonic anhydrase C)	LOC477928
3.2	1.3	5.1	0.000492	CF409176	Similar to ADAMTS-10 (A disintegrin and metalloproteinase with thrombospondin motifs 10) (ADAM-TS 10)	LOC478077
3	0.9	5.2	0.000692	AB049597.1	Epidermal growth factor	CEGF
2.7	2.2	3.3	0.00002	CO593864	Somatostatin receptor 2	SSTR2
2.4	0.4	4.3	0.000189	U16208.1	Fibronectin 1	FN1
2	1.6	2.4	0.00002	AB085580.1	Caspase-3	CASP3
2	1.9	2.1	0.00002	CO585869	Dystonin	DST
1.9	1	2.8	0.00013	AF133250.1	Vascular endothelial growth factor 188	VEGF
1.9	1.6	2.1	0.00002	CO697517	Similar to fibrinogen-like protein 1 precursor (Hepatocyte-derived fibrinogen-related protein 1) (HFREP-1) (Hepassocin) (HP-041)	LOC475617
1.9	0.6	3.2	0.000023	CO619157	Similar to basic beta 1 syntrophin	LOC482030
1.8	1	2.5	0.000027	AY305401.1	Somatostatin receptor 2	SSTR2
1.8	1.7	2	0.00002	CF411593	Similar to UDP-Gal:betaGlcNAc beta 1,4- galactosyltransferase 4	LOC487991
1.8	1.3	2.3	0.00002	CO698628	Similar to 78-kDa glucose-regulated protein precursor (GRP 78) (Immunoglobulin heavy chain-binding protein) (BiP)	LOC480726
1.7	1	2.5	0.000023	CO601750	Similar to DnaJ (Hsp40) homolog, subfamily C, member 3	LOC476966
1.7	0.5	3	0.000241	CO696669	Similar to notch1 preproprotein	LOC480676
1.6	1.1	2	0.000167	BM537581	Translocation-associated membrane protein 1	TRAM1
1.6	0.9	2.2	0.000068	CO710930	Mucin	LOC404014
1.6	1.4	1.7	0.00002	CO703865	Similar to cyclin G1 (Cyclin G)	LOC479303
1.6	1.3	1.8	0.00002	AJ407826	Similar to heat shock cognate 71 kDa protein	LOC479406
1.5	1.2	1.8	0.00002	CO715646	Similar to heat shock protein 1, beta	LOC474919
1.4	0.3	2.4	0.000692	BU744786	CD56 140 kDa isoform	LOC479435
1.4	1.2	1.7	0.00002	D38223.1	Annexin A4	ANXA4
1.4	1.1	1.7	0.00003	AF201729.1	Matrix metalloproteinase-13	MMP13
1.4	1.1	1.8	0.00002	BU751122	Similar to junctional adhesion molecule 3 precursor	LOC489271
1.4	1	1.8	0.000273	CO666324	Similar to cyclin G2	LOC478442
1.3	0.9	1.8	0.000241	CO635035	Estrogen-regulated LIV-1 protein	LIV-1
1.3	1	1.5	0.001336	AF084483.1	Muscarinic acetylcholine receptor m2	CHRM2
1.3	0.8	1.7	0.00002	CO584391	Similar to osteopontin precursor (bone sialoprotein 1) (Secreted phosphoprotein 1) (urinary stone protein) (nephropontin) (uropontin)	LOC478471
1.2	1.1	1.2	0.00002	DG8-215h9-939b11.r1ca	Fibronectin 1	FN1
1.2	0.9	1.4	0.00002	U52106.1	Fibronectin 1	FN1
1.1	0.6	1.6	0.000023	U52105.1	Fibronectin 1	FN1
1.1	0.5	1.6	0.001201	CO672418	Dystonin	DST
1.1	1	1.2	0.00002	CO675662	Metallothionein-1	LOC403800
1.1	0.3	1.9	0.000101	DG2-97k24-149d4.r1ca	Similar to pleiotrophin precursor–mouse similar to pleiotrophin precursor–mouse	LOC475509/LOC480079
1	0.8	1.1	0.00002	AF211257.1	Fibroblast growth factor receptor 2	FGFR2
1	0.8	1.2	0.00002	AF525493.1	Heat shock 27-kDa protein 8	HSPB8
1	0.5	1.4	0.000027	AF060562.1	Basic fibroblast growth factor	BFGF
1	0.8	1.2	0.00002	CO603430	Dystonin	DST
1	0.4	1.5	0.000492	CO693021	Similar to chloride intracellular channel protein 4 (mc3s5/mtCLIC)	LOC487367
1	0.8	1.1	0.000078	BM538976	Similar to 60-kDa heat shock protein, mitochondrial precursor (60 kDa chaperonin) (heat shock protein 60) (mitochondrial matrix protein P1) (P60 lymphocyte protein)	LOC478854
1	0.7	1.3	0.00002	CO625323	Similar to bone morphogenetic protein 6	LOC478715
1	-0.1	2.1	0.00003	CF407676	Similar to crystallin, ζ-like 1 isoform a	LOC478408

Shaded boxes indicate genes analyzed by RT-PCR.

Table 3. Genes With Signal Log Ratio of (−3) or Lower in the NP *Versus* AF Microarray Comparison

Signal Log Ratio	Signal Log Ratio Low	Signal Log Ratio High	Change in *P*	Representative Public ID	Gene Title	Gene Symbol
−8.9	−12.4	−5.4	0.99998	CO702793	Phosphoenolpyruvate carboxykinase	PEPCK
−7.3	−10	−4.6	0.99997	CO585446	Similar to Laminin β-1 chain precursor (Laminin B1 chain)	LOC475883
−7.2	−9.1	−5.2	0.99998	AF099154.1	Von Willebrand factor	VWF
−7.2	−9.2	−5.1	0.99998	CO698338	MHC class II DR alpha chain	DLA-DRA1
−6.9	−8.5	−5.3	0.99998	M29611.1	MHC class II DLA DRB1 beta chain	DLA-DRB1
−6.2	−7.2	−5.3	0.99998	AF153062.1	Type I collagen pre-pro-alpha1(I) chain	COL1A1
−6.1	−9.6	−2.6	0.999562	CO613060	Similar to collagen type XIV	LOC475085
−6	−6.2	−5.8	0.99998	DG14-68n1-973g20.r1ca	Type I procollagen pro-alpha 2 chain	COL1A2
−5.7	−7.9	−3.5	0.99998	BU746128	Cathepsin S	CTSS
−5.7	−7.8	−3.6	0.99998	DG14-67c3-973h12.r1ca	Similar to β-tropomyosin	LOC481598
−5.4	−7.5	−3.4	0.99998	AB011373.1	Aquaporin 1	AQP1
−5.4	−7.7	−3.1	0.999965	CO702048	Similar to CD163 antigen isoform a	LOC477704
−5.2	−7	−3.4	0.99998	U66246.1	Von Willebrand factor	VWF
−5.2	−5.8	−4.7	0.99998	CO709518	Similar to myosin light chain 3	LOC478896
−5.2	−8.1	−2.4	0.999977	CO718911	Similar to caveolin 3	LOC484671
−5.1	−5.4	−4.7	0.99998	CO709482	Myosin, light polypeptide 2, regulatory, cardiac, slow	MYL2
−5.1	−5.5	−4.6	0.99998	BU745565	Slow myosin heavy chain	MYH7
−5.1	−6.3	−3.9	0.99998	CO719197	Similar to myoglobin	LOC481283
−5.1	−5.6	−4.6	0.99998	BU745233	Similar to troponin C, slow	LOC476595
−5	−6.9	−3.1	0.999977	CO711833	Similar to Chloride intracellular channel 2	LOC492270
−4.9	−5.3	−4.4	0.99998	CO657313	Similar to hemoglobin beta chain-dog	LOC480784
−4.8	−6.9	−2.7	0.999562	CO666771	Similar to integrin α-7 precursor (UNQ406/PRO768)	LOC481097
−4.8	−7.3	−2.2	0.999954	CO598893	Similar to integrin β4 precursor (GP150) (CD104 antigen)	LOC483318
−4.6	−6.8	−2.4	0.999911	BU749834	Cardiac titin	TTN
−4.6	−5.3	−3.9	0.999932	CF412378	Myosin, light polypeptide 2, regulatory, cardiac, slow	MYL2
−4.5	−5.4	−3.7	0.99997	AF111100.1	Matrix metalloproteinase-2	MMP-2
−4.5	−6.1	−3	0.99998	BU744374	Triadin	TRDN
−4.5	−7.2	−1.7	0.99996	CO608832	Similar to collagen type XIV	LOC475085
−4.4	−6	−2.9	0.99751	CO713963	Similar to neuropilin-1 precursor (Vascular endothelial cell growth factor 165 receptor)	LOC477955
−4.2	−6.5	−1.9	0.999977	AY156692.1	Cathepsin S	CTSS
−4.2	−6.4	−1.9	0.999693	DG9-119a21-441b5.r1ca	Similar to adenylate cyclase 2	LOC480271
−4.2	−5.2	−3.2	0.99998	CO586808	Similar to fibulin 2, precursor	LOC484634
−4	−5.6	−2.5	0.999922	CO674494	Cathepsin S	CTSS
−3.6	−5.1	−2.2	0.999781	CO701916	Similar to enolase 3, beta	LOC479469
−3.5	−4.6	−2.5	0.999308	BU748808	Similar to filamin	LOC481084
−3.3	−5.1	−1.6	0.999965	U32086.1	Vascular cell adhesion molecule-1	VCAM1
−3.3	−5.3	−1.3	0.99998	BM539480	β-actin, similar to cytoplasmic β-actin	ACTB/LOC479083
−3.3	−4.2	−2.3	0.99996	AY134865.1	Cardiac titin	TTN
−3.3	−5.4	−1.2	0.999954	L08254.1	Phenylalanine hydroxylase	PAH
−3.2	−3.6	−2.9	0.99998	DG2-59i4-199b11.r1ca	Similar to alpha 1 type XII collagen long isoform precursor	LOC481881
−3	−4.8	−1.1	0.999922	L31625.1	Intercellular adhesion molecule-1	ICAM-1
−3	−3.5	−2.4	0.999977	BU744706	Collagen type IV alpha 2 chain	COL4A2
−3	−4.3	−1.7	0.999973	DG14-126l3-1074k14.r1ca	Uncoupling protein 3	UCP3

coccygeal than in lumbar AF. Comparing results obtained from dog with rat tissues, the relative *COMP* and *MGP* gene expression was similar in the dog and the rat, whereas interspecies differences were evident in the expression of *GPC3*, *PTN*, and *VIM*.

Immunohistochemistry

Basically, observations with respect to differences in gene expression were confirmed at the protein level. A strong immunopositive signal for A2M was observed in the coccygeal NP. The staining was cell-associated and mainly intracellular. Although some A2M-negative cells were seen, the majority of the NP cell clusters reacted positive for A2M. In lumbar NP, the A2M immunoreaction appeared weaker than in the coccygeal NP. Nevertheless, most lumbar NP cells also showed positive staining. However, A2M immunoreactivity was not observed in lumbar and coccygeal AF and in AC (Figure 3).

Comparing DSC2 staining in NP, AF, and AC, most immunopositive cells were noted among articular chondrocytes. Staining was cell-associated and was evident in the middle and deep zones of the cartilage. Both lumbar and coccygeal NP also had DSC2 positive cells, whereas AF tissues were immunonegative (Figure 4).

Positive staining for NCAM1 (CD56) was noticed in a small proportion of colonized lumbar NP cells. Higher numbers of colonized NP cells that reacted positively were seen in the coccygeal discs. Both AF and AC were negative for NCAM1 (CD56) (Figure 5).

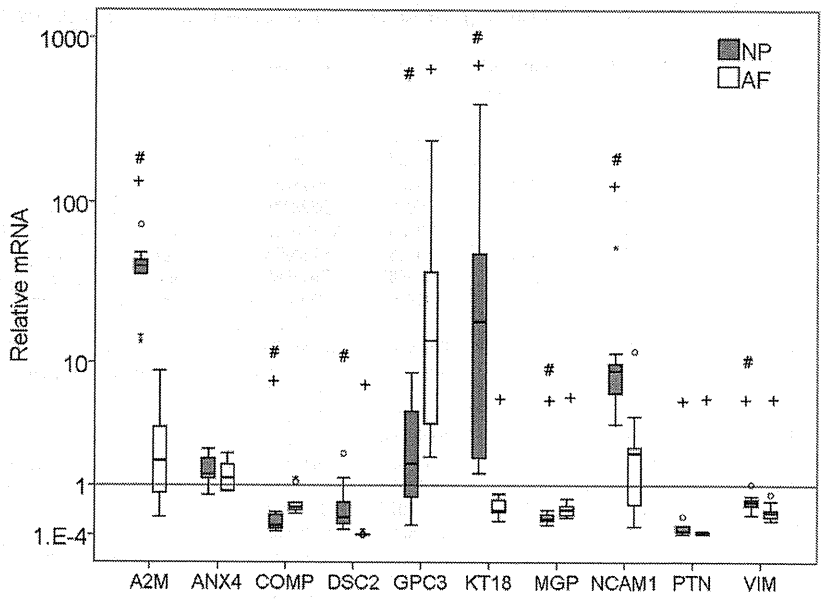

Figure 1. Relative mRNA expression of nucleus pulposus (NP) and anulus fibrosus (AF) tissue isolated from intervertebral discs of beagle dog lumbar spine. Data are expressed relative to the levels of articular cartilage (AC). $+P < 0.05$ *vs.* AC; $\#P < 0.05$ *vs.* AF; n = 9.

The expression of CK18 was visualized by immunofluorescence. A strong signal was associated with the majority of both lumbar and coccygeal NP cells. Articular chondrocytes also showed a positive reaction, although numerous cells in AC were CK18 negative. Similar results were obtained for AF cells. Generally, the CK18 staining was weaker in AF than in NP sections (Figure 6).

Immunoreactivity for GPC3 was observed only in the coccygeal AF, where the staining was localized intracellularly (Figure 7). GPC3 was not detectable in lumbar AF, NP, and AC tissues (not shown).

Discussion

With the aim to elucidate differences between different cell types present in the IVD, previous studies have addressed phenotypic characteristics and matrix production.[21,22] Whereas those investigations primarily focused on the expression and synthesis of matrix molecules such as collagens and proteoglycans, this extended study used large-scale gene expression profiling to identify differences in the expression patterns of NP and AF cells. Cartilage was included into RT-PCR and immunohistochemical examination because of the close similarities between IVD cells and articular chondrocytes.[21,22] We have previously reported on a related study using rat cells and tissues.[16] In the present study, we opted for the beagle dog because this breed is known as chondrodystrophoid, which – in contrast to the rat – lacks a notable notochordal cell population in the NP after birth and is therefore more similar to that found in humans.[23,24]

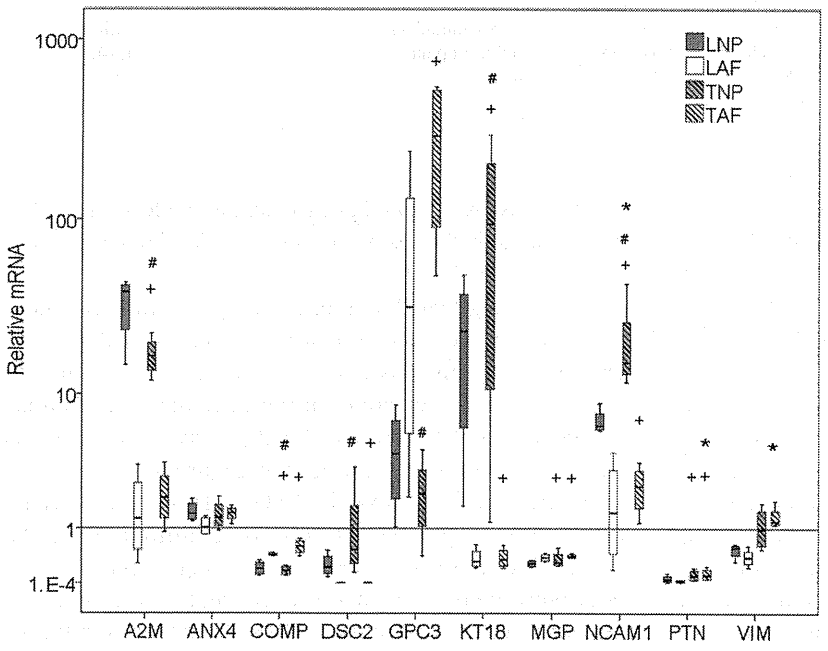

Figure 2. Relative mRNA expression of nucleus pulposus (TNP) and anulus fibrosus (TAF) tissue isolated from intervertebral discs of beagle dog tail. Expression of the corresponding lumbar disc nucleus pulposus (LNP) and anulus fibrosus (LAF) is shown for comparison. Data are expressed relative to the levels of articular cartilage (AC). $+P < 0.05$ *vs.* AC; $\#P < 0.05$ *vs.* TAF; $*P < 0.05$ *vs.* lumbar; n = 4.

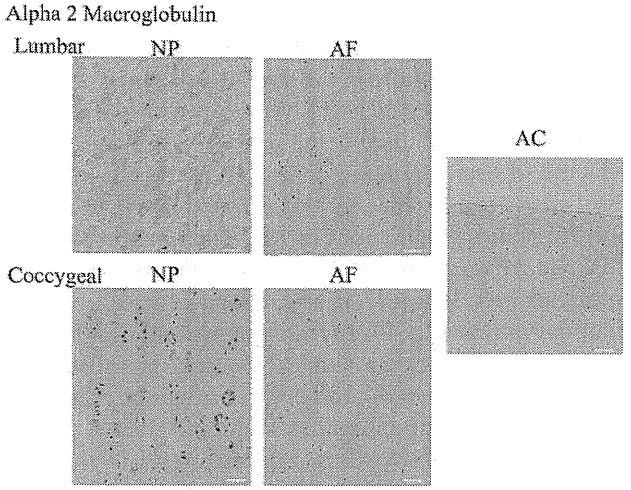

Figure 3. Immunolocalization of α-2-macroglobulin in lumbar and coccygeal nucleus pulposus (NP). The majority of NP cells stain positive, whereas lumbar and coccygeal anulus fibrosus (AF) and articular cartilage (AC) cells are immunonegative. Scale bars: 200 μm.

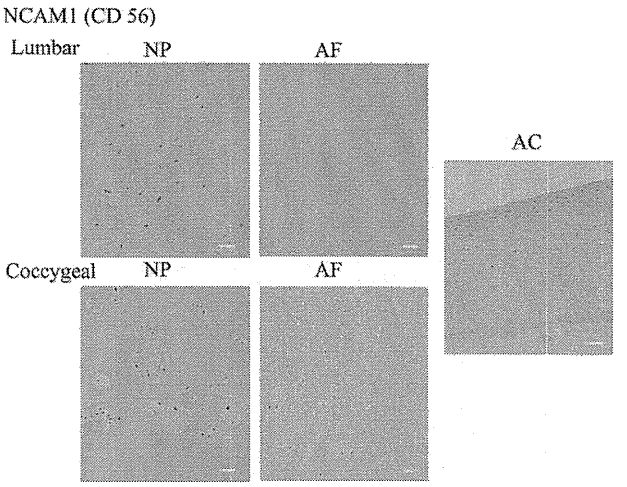

Figure 5. Immunolocalization of neural cell adhesion molecule 1 (CD56) in lumbar and coccygeal nucleus pulposus (NP). The majority of coccygeal and a smaller proportion of lumbar NP cells stain positive, whereas lumbar and coccygeal anulus fibrosus (AF) and articular cartilage (AC) cells are immunonegative. Scale bars: 200 μm.

In this microarray analysis of mature female beagle dogs, 45 genes were found with a high ($\geq$1) NP/AF signal log ratio, whereas 77 genes had a low (≤ -1) NP/AF ratio. Even though these data originate from 3 independent microarray analyses, they can be considered neither as comprehensive nor conclusive. The aim was to identify potential candidate genes that were further investigated by quantitative RT-PCR. The selection for RT-PCR was primarily focused on genes with a high NP/AF signal ratio in the microarray. Generally, results from the microarray analysis were confirmed at gene expression and for the most part also at protein levels. However, although ANXA4 was expressed significantly more highly in NP compared to AF in the microarray analysis, this difference could not be confirmed by real-time RT-PCR. It is important to consider that with the capability to screen large proportions of a genome, microarrays have the disadvantages of a certain lack in both sensitivity and specificity, which is associated with a considerable proportion of false positives.[25,26] Possible reasons for the disagreement between microarray and quantitative RT-PCR may include recognition of alternative transcripts, cross-hybridization, and signal quantification techniques, among others. Furthermore, different animals, although of the same age and sex, were used for microarray and RT-PCR analysis, which may also account for the observed divergences. Taken together, this

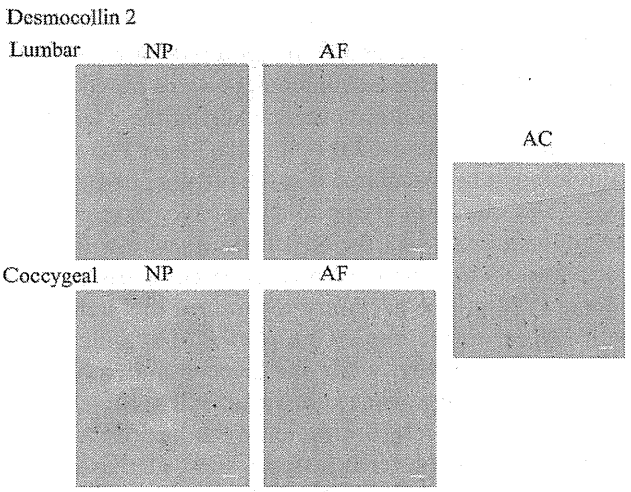

Figure 4. Immunolocalization of desmocollin-2 in lumbar and coccygeal nucleus pulposus (NP) and in articular cartilage (AC). Cartilage and a proportion of NP cells stain positive, whereas anulus fibrosus (AF) cells are immunonegative. Scale bars: 200 μm.

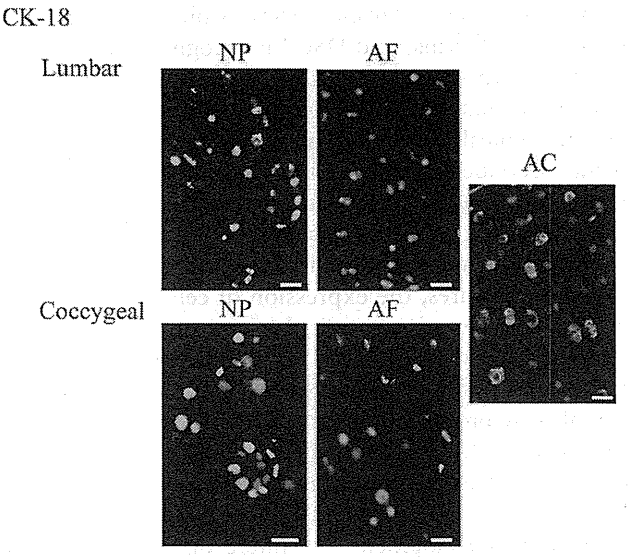

Figure 6. Immunostaining of cytokeratin-18 in lumbar and coccygeal nucleus pulposus (NP) and anulus fibrosus (AF) and in articular cartilage (AC) cells. The majority of lumbar and coccygeal NP cells stain strongly positive, whereas AF and AC cell staining is weaker or negative. Scale bars: 100 μm.